Journal of Inflammation Research

Dovepress
Taylor & Francis Group

Open Access Full Text Article

ORIGINAL RESEARCH

Integrating Network Pharmacology and in vivo Validation to Explore the Mechanisms of Buyang Huanwu Decoction in Myocardial Ischemia-Reperfusion Injury

Yushan Luo[1], Wen Hu[1], Ziyue Li[1], Xiaoyuan Zhang[1], Shoujun Chen[1], Qiang Yang[1], Bailong Hu[2], Xiaohua Zou[2]

[1]Guizhou Medical University, Guiyang, Guizhou, 550004, People's Republic of China; [2]Department of Anesthesiology, The Affiliated Hospital of Guizhou Medical University, Guiyang, Guizhou, 550004, People's Republic of China

Correspondence: Bailong Hu; Xiaohua Zou, Department of Anesthesiology, Affiliated Hospital of Guizhou Medical University, Guiyang, Guizhou, People's Republic of China, Tel +86-15185184309; +86-13809416036, Fax +86-851-86771013, Email hubailong@gmc.edu.cn; zouxiaohuazxh@sina.com

Objective: Buyang Huanwu Decoction (BYHWD), a traditional Chinese herbal formula, has been widely used to manage cardiovascular disorders. However, its cardioprotective mechanisms in myocardial ischemia/reperfusion injury (MI/RI) remain unclear. This study aims to investigate its pharmacological mechanisms against MI/RI through network pharmacology and experimental validation.

Materials and Methods: Active components and targets of BYHWD were identified via Traditional Chinese Medicine Systems Pharmacology Database and Analysis Platform, Encyclopedia of Traditional Chinese Medicine, BATMAN-TCM, and SymMap databases. MI/RI-related targets were retrieved from DisGeNET, GeneCard, Online Mendelian Inheritance in Man, Comparative Toxicogenomics Database, and DrugBank databases. The intersecting targets were analyzed using Gene Ontology (GO) and Kyoto Encyclopedia of Genes and Genomes (KEGG) enrichment. Protein-protein interaction (PPI) networks, compound-target networks, and herb-target-pathway networks were constructed using Cytoscape, and molecular docking was performed via AutoDock Vina. A rat MI/RI model was used to assess infarct size, protein expression, and cytokine levels for in vivo validation.

Results: 95 compounds were identified, with 75 MI/RI-related targets. PPI analyses highlighted ten hub genes, including interleukin-6 (IL6), AKT serine/threonine kinase 1 (AKT1), tumor necrosis factor (TNF), intercellular adhesion molecule 1 (ICAM1), matrix metalloproteinase 9 (MMP9), interleukin-10 (IL10), vascular cell adhesion molecule 1 (VCAM1), nitric oxide synthase 3, albumin, and C-reactive protein. GO and KEGG analyses highlighted TNF signaling, apoptosis, and p53 signaling pathways. *Carthami Flos* and *Radix Astragali* emerged as core herbs, with *quercetin, kaempferol, baicalein, stigmasterol, baicalin*, and *beta-sitosterol* as key compounds exhibiting strong binding affinities to hub genes. In vivo, BYHWD significantly reduced myocardial infarct size, decreased inflammatory cytokines (IL6 and TNF-α), ICAM1, VCAM1, and MMP9 protein expression, and IL10 and phosphorylated AKT1 expression.

Conclusion: BYHWD alleviates MI/RI through multicomponent, multitarget, and multipathway mechanisms, primarily modulating TNF and AKT1-mediated inflammatory/apoptotic pathways. These effects collectively support its potential as a complementary treatment for ischemic heart disease.

Keywords: Buyang Huanwu decoction, myocardial ischemia reperfusion injury, network pharmacology

Introduction

Acute myocardial infarction (AMI) remains a leading cause of morbidity and mortality worldwide,[1] representing a significant health and economic burden on society.[2] Timely reperfusion and revascularization therapies, including thrombolytic agents, percutaneous coronary intervention (PCI), and coronary artery bypass grafting, are effective in

Received: 1 January 2025
Accepted: 28 May 2025
Published: 10 June 2025

restoring blood flow to the ischemic myocardium.[3] However, reperfusion itself can lead to further myocardial injury, a phenomenon known as myocardial ischemia/reperfusion injury (MI/RI).[4] The underlying mechanisms of MI/RI are multifaceted and involve calcium overload, apoptosis, oxidative damage, mitochondrial dysfunction, and inflammation.[5] The inflammatory response is vital in MI/RI, with miR-24 mitigating this by blocking the S100A8/TLR4/MyD88/NF-κB pathway,[6] thus enhancing heart function. Additionally, apoptosis and ferroptosis are crucial in MI/RI.[7] Uncoupling Protein 2 (UCP2) reduces MI/RI by inhibiting ferroptosis, possibly via the p53/TfR1 pathway.[7] Honokiol protects the heart by activating the PI3K/AKT pathway and preventing mitochondrial apoptosis.[8] Despite ongoing research, there is currently no effective treatment to prevent or manage MI/RI.[9] In recent years, the focus of medical research has shifted toward finding effective strategies to prevent and reduce MI/RI, with growing evidence supporting traditional Chinese medicine (TCM) offer a promising complementary approach to MI/RI management.[10–12]

Buyang Huanwu Decoction (BYHWD), a formula comprising *Radix Astragali, Angelicae Sinensis Radix, Radix Paeoniae Rubra, Chuanxiong Rhizoma, Carthami Flos, Persicae Semen*, and *Pheretima*, has been widely used for its vascular protective properties.[13] Research has demonstrated that BYHWD offers cerebral protection in both humans and animals.[14,15] BYHWD has demonstrated potential in improving myocardial perfusion, reducing infarct size, and alleviating angina.[16,17] Furthermore, studies suggest that BYHWD exerts its therapeutic effects by modulating angiogenesis through pathways such as Cav-1/VEGF.[18] Importantly, BYHWD demonstrates substantial clinical efficacy in the management of myocardial ischemia-reperfusion injury. A plethora of studies have indicated that BYHWD significantly attenuates the expression of inflammatory mediators,[19] reduces cardiomyocyte apoptosis,[20] enhances myocardial energy metabolism,[21] thereby augmenting myocardial repair capacity and improving cardiac function. Studies indicate that *Radix Astragali* protects cardiomyocytes from MI/RI by reducing oxidative stress and inflammation.[22] *Angelicae Sinensis Radix* enhances blood circulation and reduces ischemia-reperfusion injury by improving vascular endothelial function.[20] *Chuanxiong Rhizoma* inhibits platelet aggregation and improves microcirculation, while *Carthami Flos* offers protection through its antioxidant and anti-inflammatory properties.[14] Additionally, components like *Pheretima* and *Persicae Semen* support cardiomyocyte survival and regeneration by modulating signaling pathways such as PI3K/Akt and HIF-1.[20] Consequently, BYHWD exhibits multiple protective mechanisms in the treatment of myocardial ischemia-reperfusion injury, positioning it as a promising candidate within traditional Chinese medicine for MI/RI therapy.

Despite its long-standing clinical use, the precise molecular mechanisms underlying BYHWD's protective effects on MI/RI remain poorly understood. Given the complexity of MI/RI pathogenesis and the multi-component nature of TCM formulations, targeting a single pathway or gene is insufficient to fully elucidate its therapeutic effects. Network pharmacology, a systems biology approach that integrates multi-target pharmacology with bioinformatics, provides a powerful tool to unravel the intricate mechanisms of TCM.[23,24] This method allows us to examine the complex interactions between BYHWD's compounds, their targets, and the relevant biological pathways, providing insights that cannot be achieved by traditional pharmacological approaches. This study combines network pharmacology with experimental validation to systematically explore the molecular mechanisms by which BYHWD exerts its protective effects in MI/RI. Our findings offer a scientific basis for the clinical use of BYHWD in ischemic heart disease and provide insights into its multi-target therapeutic potential. A comprehensive workflow of the study is presented in Figure 1.

Materials and Methods

Network Pharmacology Analysis

Collection of BYHWD-Related Targets and MI/RI-Related Targets

We collected BYHWD compounds from several databases, including the TCMSP,[25] ETCM,[26] BATMAN-TCM,[27] and SymMap database.[28] Next, active components of BYHWD were screened based on absorption, distribution, metabolism, and excretion (ADME) properties, adhering to the criteria of oral bioavailability (OB) ≥ 30% and drug-likeness (DL) ≥ 0.18.[29] Information on the corresponding target proteins for these active compounds was retrieved, and the target protein names were mapped to official gene symbols through the UniProt database.[30] The target gene data were then consolidated and de-duplicated to generate a list of BYHWD-associated targets.

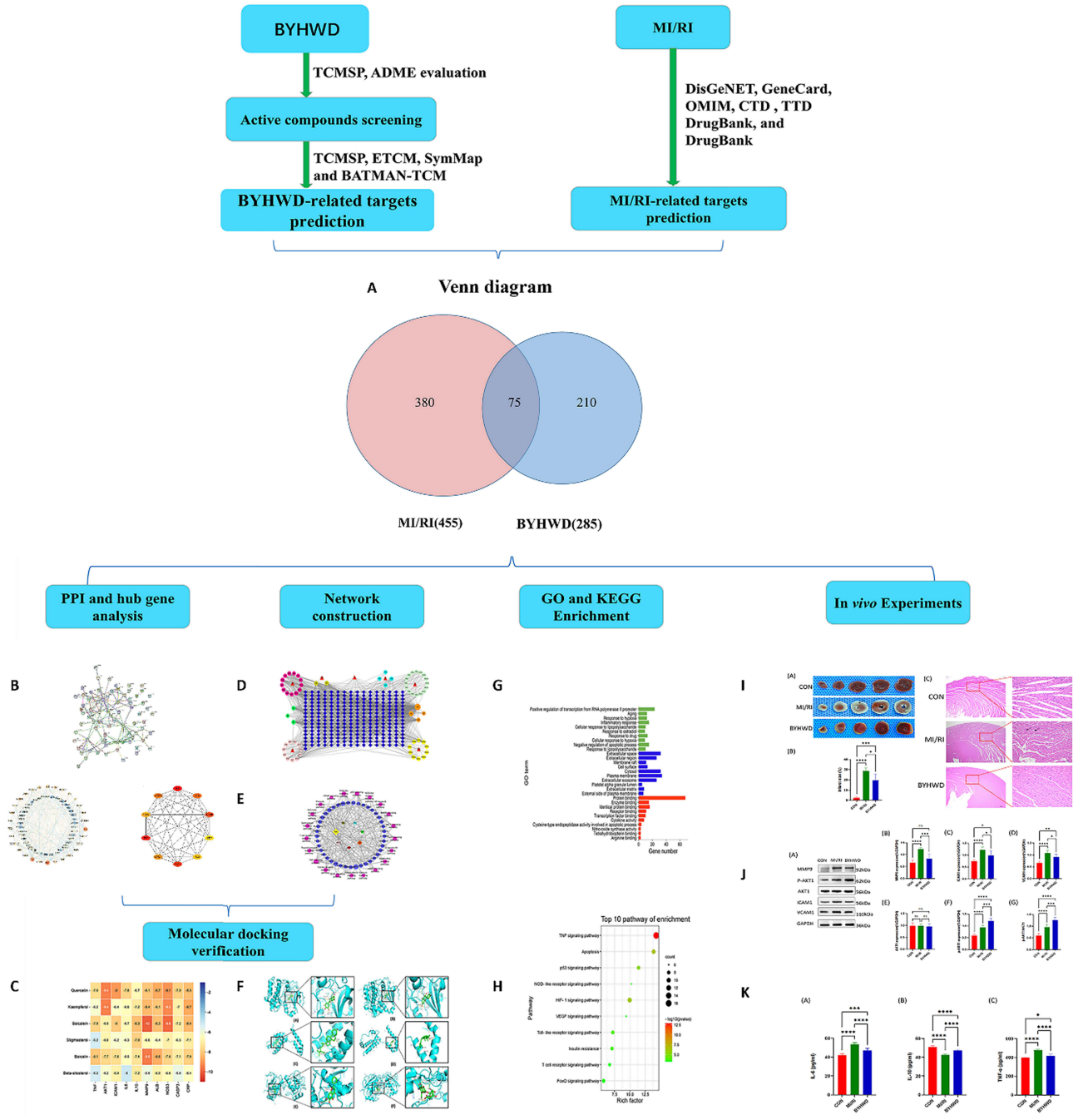

Figure 1 Flowchart of the integrated strategy for investigating BuYang HuanWu Decoction (BYHWD) against myocardial ischemia/reperfusion injury (MI/RI). (**A**) Venn diagram for BYHWD-related targets and MI/RI-related targets; (**B**) Protein-protein interaction (PPI) network and top 10 hub genes for BYHWD anti-MI/RI; (**C**) Heatmap of molecular docking scores; (**D**) Herb-compound-target network; (**E**) Herb-target-pathway network; (**F**) Molecular docking between hub genes and key active compounds; (**G**) Gene Ontology (GO) enrichment analysis; (**H**) Kyoto Encyclopedia of Genes and Genomes (KEGG) pathway enrichment analysis; (**I**) Effect of BYHWD on myocardial infarction size and hematoxylin-eosin (HE) staining; (**J**) Effect of BYHWD on protein expression of hub genes; (**K**) Effect of BYHWD on inflammatory cytokine expression. *p < 0.05, **p < 0.01, ***p < 0.001, ****p < 0.0001.
Abbreviation: ns, not significant.

For MI/RI-related targets, we extracted data from seven publicly available databases: DisGeNET,[31] GeneCard,[32] OMIM,[33] Comparative Toxicogenomics Database (CTD),[34] TTD,[35] DrugBank,[36] and MalaCards.[37] Using the keyword "myocardial ischemia reperfusion injury", the targets identified were aggregated, unified, and filtered for duplicates to produce a comprehensive list of MI/RI-associated genes.

https://doi.org/10.2147/JIR.S512050

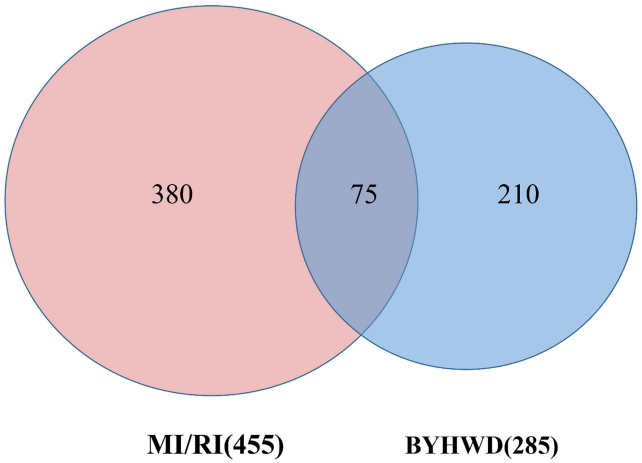

Figure 2 Venn diagram for BuYang HuanWu Decoction (BYHWD)-related targets and myocardial ischemia/reperfusion injury (MI/RI)-related targets.

Collection of Potential Common Targets for BYHWD Against MI/RI

The potential intersection targets of BYHWD and MI/RI were obtained and drawn using Venn (Figure 2).

Protein-Protein Interaction (PPI) Network Construction and Hub Gene Analysis

The intersection targets of BYHWD and MI/RI were analyzed using String 11.5[38] to construct a PPI network and a minimum confidence score of 0.7 was applied to ensure high reliability of the interactions. The PPI network result was visualized using Cytoscape software. Hub genes were identified using the CytoHubba plugin within Cytoscape, based on the maximum clique centrality (MCC) algorithm.

Gene Ontology (GO) and Pathway Enrichment

We used the DAVID database[39] for annotation of GO and Kyoto Encyclopedia of Genes and Genomes (KEGG) pathway enrichment. The pathway maps were further visualized through an online tool[40] to enhance interpretability.

Network Construction

Data on BYHWD-MI/RI targets, active compounds, key signaling pathways and herbs were integrated into Cytoscape to construct and refine two networks: (1) the compound-target network of treatment with BYHWD for MI/RI, and (2) the herb-target pathway network of treatment with BYHWD for MI/RI.

Molecular Docking Verification

To confirm compound-target interactions, molecular docking was conducted using AutoDock Vina.[41] The selected active compounds were used as ligands, while the top 10 hub genes served as receptors. Three-dimensional crystal structures of the hub genes were retrieved from the RCSB Protein Data Bank,[42] and the MOL2 files of the active compounds were obtained from PubChem.[43] Protein preparations involved removing water molecules, adding polar hydrogens, and merging nonpolar hydrogens, followed by conversion to PDBQT format. The docking results, visualized with PyMOL,[44] evaluated binding affinity, with a binding energy below −5 kcal/mol indicating strong interactions.[45]

In vivo Experiment Validation

Reagent

BYHWD, consisting of *Radix Astragali, Angelicae Sinensis Radix, Radix Paeoniae Rubra, Chuanxiong Rhizoma, Carthami Flos, Persicae Semen*, and *Pheretima* at a dispensing ratio of 120:10:10:10:10:10:4.5 (dry weight), was purchased from the affiliated hospital of Guizhou Medical University. The preparation and quality control of BYHWD were performed according to previously established methods.[46] For Western blot analysis, the following primary antibodies were used: anti-MMP-9, anti-AKT1, anti-ICAM1, anti-VCAM1, and anti-phospho-AKT. GAPDH was used as a loading control. Secondary antibodies were matched appropriately with the host species of the primary antibodies

and were used at the dilutions recommended by the manufacturers (Antibody information is provided in the Supplementary Table).

Animal Model and Treatment

Male Sprague-Dawley rats (200 ± 20 g, aged 5–6 weeks) were purchased from Changsha Tianqin Bioscience Co., Ltd. (certificate no. SCXK (Xiang) 2022–0011) and randomly assigned to sham, MI/RI, and MI/RI + BYHWD groups (n=10 per group). The study was approved by the Animal Ethics Committee of the Guizhou Medical University (Approval No. 2305219). The MI/RI model was established by occluding the left anterior descending (LAD) coronary artery for 30 minutes, followed by 2 hours of reperfusion. Briefly, rats were anesthetized with an intraperitoneal injection of 2% sodium pentobarbital (50 mg/kg body weight). The chest cavity was exposed through a midline sternotomy, and the heart was carefully exteriorized. The LAD coronary artery was located, and a 6–0 silk suture was passed around the artery. The suture was tightened to achieve ischemia, confirmed by a change in the myocardial color to a pale gray or cyanotic appearance and a ST-segment elevation on electrocardiogram (ECG). After 30 minutes of ischemia, the suture was released to allow reperfusion for 2 hours. Rats in the BYHWD group were orally administered BYHWD (12.84 g/kg/day) for three weeks before ischemia induction.[16] The sham group underwent the surgical procedure without LAD ligation. ECG monitoring was continuously conducted to assess changes in real time. LAD ligation resulted in myocardial discoloration (gray or cyanotic appearance) and ST-segment elevation on ECG, which confirmed successful ischemia. Reperfusion was indicated by more than 50% reduction in ST-segment elevation.

Following reperfusion, animals were euthanized by overdose of isoflurane anesthesia and cervical dislocation. The heart was immediately excised, placed in cold phosphate-buffered saline (PBS), and then snap frozen in liquid nitrogen for further analysis. The frozen heart tissues were stored at −80°C until further processing for protein expression.

Assessment of Myocardial Infarction Size

Myocardial infarction size was assessed via triphenyltetrazolium chloride (TTC) staining. Immediately after reperfusion and heart excision, the hearts were then frozen at −20°C for 10–15 min and transversely sectioned into 1–2 mm thick slices from the apex to the base. Frozen heart tissue slices were then incubated in TTC (1%, 5 mL) solution at 37°C for 30 minutes in the dark. The infarcted regions, which lacked TTC reduction, appeared white or pale, whereas the non-infarcted areas, which retained the TTC, appeared red. Myocardial infarct size was calculated using Image-Pro Plus software (Media Cybernetics), with the following formula: infarct size (%) = (infarct area/total heart area) × 100%.

Histopathology

For histopathological examination, the myocardial tissue was fixed in 4% paraformaldehyde, dehydrated in ethanol, embedded in paraffin, and sectioned. Hematoxylin and eosin (H&E) staining was performed, and histopathological changes were examined under a light microscope at 200× magnification. The images were captured using the BA210 Digital Trinocular Camera Microscopy System from Motic Industrial Group Co., Ltd. (China).

ELISA

Serum concentrations of cytokines, including IL-6, IL-10, and TNF-α, were measured using quantitative ELISA kits according to the manufacturer's instructions. Briefly, 50 μL of serum sample was added to pre-coated ELISA plates, followed by incubation at room temperature for 2 hours to allow the cytokines to bind to the capture antibody. After incubation, the plates were washed three times with washing buffer to remove unbound substances. HRP-conjugated secondary antibody was then added and incubated at room temperature for 1 hour. After another wash, the substrate solution was added, and a colorimetric reaction was allowed to develop. The optical density was measured at 450 nm using a microplate reader. Cytokine concentrations were determined using a standard curve constructed for each cytokine.

Blood was collected from the tail vein of each animal, and approximately 1–2 mL of blood was obtained per animal. The blood was allowed to clot at room temperature for 30 minutes and then centrifuged at 1500 rpm for 10 minutes. The serum was carefully separated and stored at −80°C until further analysis.

Western Blot

Proteins were extracted from myocardial tissue obtained from the apex of left ventricle using RIPA buffer (Thermo Scientific), and concentrations were measured with a BCA Protein Assay Kit (Thermo Fisher Scientific, P0010). Proteins were separated by SDS-PAGE, transferred to PVDF membranes, blocked with 5% milk, and incubated with primary antibodies (AKT, phospho-AKT, ICAM1, VCAM1, MMP9, and GAPDH) overnight. After washing, membranes were treated with HRP-conjugated secondary antibodies, and protein expression was visualized using enhanced chemiluminescence (ECL). Protein expression levels were quantified using Image Lab software and normalized to GAPDH.

Statistical Analysis

Statistical analysis was performed using SPSS software (Version 25, IBM Corp., USA). Data are expressed as mean ± standard deviation. For normally distributed data, one-way ANOVA followed by Bonferroni post-hoc tests was used. Statistical significance was set at $p < 0.05$.

Results

Targets of BYHWD and MI/RI

A total of 794 compounds were initially identified across the seven herbal components of Buyang Huanwu Decoction (BYHWD): *Radix Astragali* (87 compounds), *Angelicae Sinensis Radix* (125 compounds), *Chuanxiong Rhizoma* (189 compounds), *Radix Paeoniae Rubra* (119 compounds), *Persicae Semen* (66 compounds), *Carthami Flos* (189 compounds), and *Pheretima* (19 compounds). Applying the ADME criteria (OB ≥ 30%, DL ≥ 0.18), 106 potential compounds from the seven herbal medicines in BYHWD were screened. Of these, 95 were identified as potential active compounds, which is provided in Table 1. Subsequently, the UniProt database was used to identify and verify the target protein names of these compounds and their corresponding gene names. This process resulted in the identification of 285

Table 1 Active Compounds of BYHWD and Their Parameters

Mol ID	Compound Name (Key Function)	Source Herbs	OB(%)	DL	Overlap Status
MOL000006	luteolin	CF	36.16	0.246	Unique to CF
MOL000033	(3S,8S,9S,10R.phenanthren-3-ol)	RA	36.23	0.783	Unique to RA
MOL000098	quercetin	RA	46.43	0.275	Unique to RA
MOL000211	Mairin	RA	55.38	0.776	Unique to RA
MOL000239	Jaranol	RA	50.83	0.291	Unique to RA
MOL000296	hederagenin	RA	36.91	0.751	Unique to RA
MOL000358	beta-sitosterol	ASR, RPR	36.91	0.751	**Shared**
MOL000359	sitosterol	CR	36.91	0.751	Unique to CR
MOL000433	FA	RA, CR	68.96	0.706	**Shared**
MOL000438	(3R)-3-(2-hydroxy-3.chroman-7-ol)	RA	67.67	0.265	Unique to RA
MOL000439	Isomucronulatol-7,2′-di-O-glucosiole	RA	49.28	0.621	Unique to RA
MOL000449	Stigmasterol	ASR, RPR	43.83	0.757	**Shared**
MOL000492	(+)-catechin	RPR	54.83	0.242	Unique to RPR
MOL000493	campesterol	PS	37.58	0.715	Unique to PS
MOL001002	Ellagic acid	RPR	43.06	0.434	Unique to RPR
MOL001323	Sitosterol alpha1	PS	43.28	0.784	Unique to PS
MOL001494	Mandenol	CR	42.00	0.193	Unique to CR
MOL001918	paeoniflorgenone	RPR	87.59	0.367	Unique to RPR
MOL001921	Lactiflorin	RPR	49.12	0.797	Unique to RPR
MOL001924	paeoniflorin	RPR	53.87	0.787	Unique to RPR
MOL002135	Myricanone	CR	40.60	0.513	Unique to CR
MOL002140	Perlolyrine	CR	65.95	0.275	Unique to CR

(*Continued*)

Table 1 (Continued).

Mol ID	Compound Name (Key Function)	Source Herbs	OB(%)	DL	Overlap Status
MOL002151	senkyunone	CR	47.66	0.244	Unique to CR
MOL002157	wallichilide	CR	42.31	0.706	Unique to CR
MOL002694	4-[(E)−4−(3,5−dimethoxy.)] [(*E*)−4−(3,5−*dimethoxy.*)]	CF	48.47	0.365	Unique to CF
MOL002776	Baicalin	RPR	40.12	0.753	Unique to RPR
MOL002883	Ethyl oleate	RPR	32.40	0.191	Unique to RPR
MOL004355	Spinasterol	RPR	42.98	0.755	Unique to RPR
MOL005043	campest-5-en-3beta-ol	RPR	37.58	0.715	Unique to RPR
MOL001439	Arachidonic Acid	Ph	45.57	0.200	Unique to Ph

Abbreviations: RA, *Radix Astragali*; ASR, *Angelicae Sinensis Radix*; CR, *Chuanxiong Rhizoma*; RPR, *Radix Paeoniae Rubra*; PS, *Persicae Semen*; CF, *Carthami Flos*; Ph, *Pheretima*; OB, *Oral Bioavailability*; DL, *Drug Likeness*.

unique BYHWD-related targets after integration and deduplication. Additionally, 455 targets associated with myocardial ischemia/reperfusion injury (MI/RI) were identified using seven databases: DisGeNET, OMIM, CTD, TTD, GeneCards, DrugBank, and MalaCards. A Venn diagram revealed 75 overlapping genes between the BYHWD and MI/RI target datasets. These common targets are listed in Table 2 and visually represented in Figure 2.

Table 2 Determined Target Information of BYHWD Related to MI/RI

UniProt ID	Gene Name	Protein Name
P35228	NOS2	Nitric oxide synthase, inducible
Q14432	PDE3A	cGMP-inhibited 3′,5′-cyclic phosphodiesterase A
P03372	ESR1	Estrogen receptor
Q16539	MAPK14	Mitogen-activated protein kinase 14
P11309	PIM1	Proto-oncogene serine/threonine-protein kinase Pim-1
P11217	PYGM	Glycogen phosphorylase, muscle form
P15121	AKR1B1	Aldo-keto reductase family 1 member B1
P08709	F7	Coagulation factor VII
P00734	F2	Prothrombin
P29474	NOS3	Nitric-oxide synthase, endothelial
P78380	OLR1	Oxidized low-density lipoprotein receptor 1
P08588	ADRB1	Beta-1 adrenergic receptor
P07550	ADRB2	Beta-2 adrenergic receptor
P35968	KDR	Vascular endothelial growth factor receptor 2
Q96EB6	SIRT1	NAD-dependent deacetylase sirtuin-1
P31749	AKT1	RAC-alpha serine/threonine-protein kinase
P10415	BCL2	Apoptosis regulator Bcl-2
Q07812	BAX	Apoptosis regulator BAX
P01375	TNF	Tumor necrosis factor
P42574	CASP3	Caspase-3
P09601	HMOX1	Heme oxygenase 1
P08684	CYP3A4	Cytochrome P450 3A4
P05362	ICAM1	Intercellular adhesion molecule 1
P16581	SELE	E-selectin
P19320	VCAM1	Vascular cell adhesion protein 1

(*Continued*)

https://doi.org/10.2147/JIR.S512050

Table 2 (Continued).

UniProt ID	Gene Name	Protein Name
P28161	GSTM2	Glutathione S-transferase Mu 2
P24385	CCND1	G1/S-specific cyclin-D1
P55211	CASP9	Caspase-9
P08253	MMP2	72 kDa type IV collagenase
P14780	MMP9	Matrix metalloproteinase-9
P05121	IL10	Interleukin-10
P05231	IL6	Interleukin-6
P25963	NFKBIA	NF-kappa-B inhibitor alpha
Q14790	CASP8	Caspase-8
P00441	SOD1	Superoxide dismutase [Cu-Zn]
Q9NWT6	HIF1A	Hypoxia-inducible factor 1-alpha
P13726	F3	Tissue factor
P17302	GJA1	Gap junction alpha-1 protein
P01137	TGFB1	Transforming growth factor beta-1
P00750	PLAT	Tissue-type plasminogen activator
P07204	THBD	Thrombomodulin
P05121	SERPINE1	Plasminogen activator inhibitor 1
P05121	PTEN	Phosphatidylinositol-3,4,5-trisphosphate 3-phosphatase and dual-specificity protein phosphatase PTEN
P01583	IL1A	Interleukin-1 alpha
P09874	PARP1	Poly [ADP-ribose] polymerase 1
P02461	COL3A1	Collagen alpha-1(III) chain
P19875	CXCL2	C-X-C motif chemokine 2
Q07869	PPARA	Peroxisome proliferator-activated receptor alpha
Q00613	HSF1	Heat shock factor protein 1
P02741	CRP	C-reactive protein
P02778	CXCL10	C-X-C motif chemokine 10
P10451	SPP1	Osteopontin
Q86XT9	IGFBP3	Insulin-like growth factor-binding protein 3
P29965	CD40LG	CD40 ligand
P10914	IRF1	Interferon regulatory factor 1
P52789	HK2	Hexokinase-2
O95644	NFATC1	Nuclear factor of activated T-cells, cytoplasmic 1
Q01469	FABP5	Fatty acid-binding protein 5
P02768	ALB	Albumin
P35222	CTNNB1	Catenin beta-1
P55210	CASP7	Caspase-7
P05067	APP	Amyloid-beta precursor protein
P05305	EDN1	Endothelin-1
P06858	LPL	Lipoprotein lipase
P55851	UCP2	Mitochondrial uncoupling protein 2
P00747	PLG	Plasminogen
P29475	NOS1	Nitric oxide synthase, brain
Q12879	GRIN2A	Glutamate receptor ionotropic, NMDA 2A
P48443	RXRG	Retinoic acid receptor RXR-gamma
P11413	G6PD	Glucose-6-phosphate 1-dehydrogenase
P47712	PLA2G4A	Cytosolic phospholipase A2
P16109	SELP	P-selectin
P05091	ALDH2	Aldehyde dehydrogenase, mitochondrial
P20333	TNFRSF1B	Tumor necrosis factor receptor superfamily member 1B
O95069	KCNK2	Potassium channel subfamily K member 2

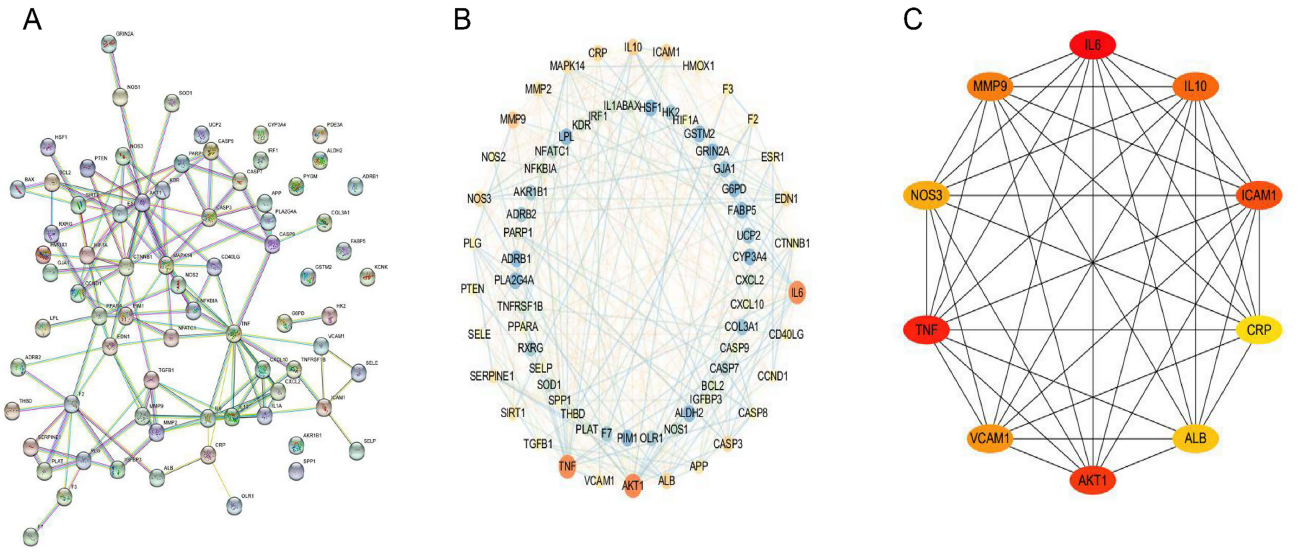

Figure 3 Protein-protein interaction (PPI) network and top 10 hub genes for BuYang HuanWu Decoction (BYHWD) anti-myocardial ischemia/reperfusion injury (MI/RI). (**A**) PPI network constructed with STRING database. (**B**) PPI network constructed with Cytoscape software (the darker the node color, the higher the number of connected proteins). (**C**) Top 10 hub genes for BYHWD anti-MI/RI were obtained by using the CytoHubba plug-in.

BYHWD-MI/RI PPI Network and Hub Genes Analysis

The 75 intersecting targets were analyzed using the STRING database, and their interaction network was visualized in Cytoscape 3.7.2. The network consists of 72 nodes and 342 edges (Figure 3A and B), with pink nodes indicating higher connectivity. The top 10 genes based on MCC algorithm are shown in Table 3, with IL6 having the highest score. Using the CytoHubba plugin and MCC algorithm, the top hub genes associated with BYHWD's effects in MI/RI were identified: IL6, AKT1, TNF, ICAM1, MMP9, IL10, VCAM1, NOS3, ALB, and CRP (Figure 3C).

Table 3 The Top 10 Genes Based on MCC Method

Rank	Gene	Score
1	IL6	20262
2	TNF	19172
3	AKT1	13541
4	ICAM1	12192
5	IL10	10776
6	MMP9	10404
7	VCAM1	7344
8	NOS3	7324
9	ALB	5864
10	CRP	5092

Abbreviations: IL6, Interleukin 6; TNF, Tumor Necrosis Factor; AKT1, AKT serine/threonine kinase 1; ICAM1, Intercellular Adhesion Molecule 1; IL10, Interleukin 10; MMP9, Matrix Metalloproteinase 9; VCAM1, Vascular cell adhesion protein 1; NOS3, Nitric Oxide Synthase 3; ALB, Albumin; CRP, C-Reactive Protein.

https://doi.org/10.2147/JIR.S512050

Gene Ontology and Pathway Enrichment Analysis

GO analysis was conducted to classify the biological processes (BP), cellular components (CC), and molecular functions (MF) associated with the 75 overlapping targets. A total of 349 GO terms were enriched, including 276 BP, 29 CC, and 44 MF terms, all with $p < 0.05$. The top 10 terms in each category are summarized in Figure 4 and Table 4. KEGG pathway analysis identified 80 enriched pathways, of which 25 were closely linked to MI/RI based on a PubMed literature review. The top pathways include TNF, apoptosis, p53, NOD-like receptor, HIF-1, and VEGF signaling pathways (Figure 5 and Table 5).

Compound-Target Network Analysis

A compound-target interaction network was constructed using Cytoscape, comprising 327 nodes and 1336 edges. The compounds with the highest degree centrality included *quercetin, kaempferol, baicalein, stigmasterol, baicalin, beta-sitosterol, luteolin, hederagenin, 3,9-di-O-methylnissolin*, and *oleic acid* (Figure 6).

Herb-Target-Pathway Network

By inputting 75 targets that intersected with MI/RI genes into the DAVID database, we identified 80 pathways associated with MI/RI. After searching the PubMed database and comparing these results with the 80 enriched pathways, 25 pathways were confirmed to be significantly enriched in relation to MI/RI. The herb-target-pathway network analysis identified *Radix Astragali* and *Carthami Flos* as the primary contributors to BYHWD's anti-MI/RI effects, with the TNF

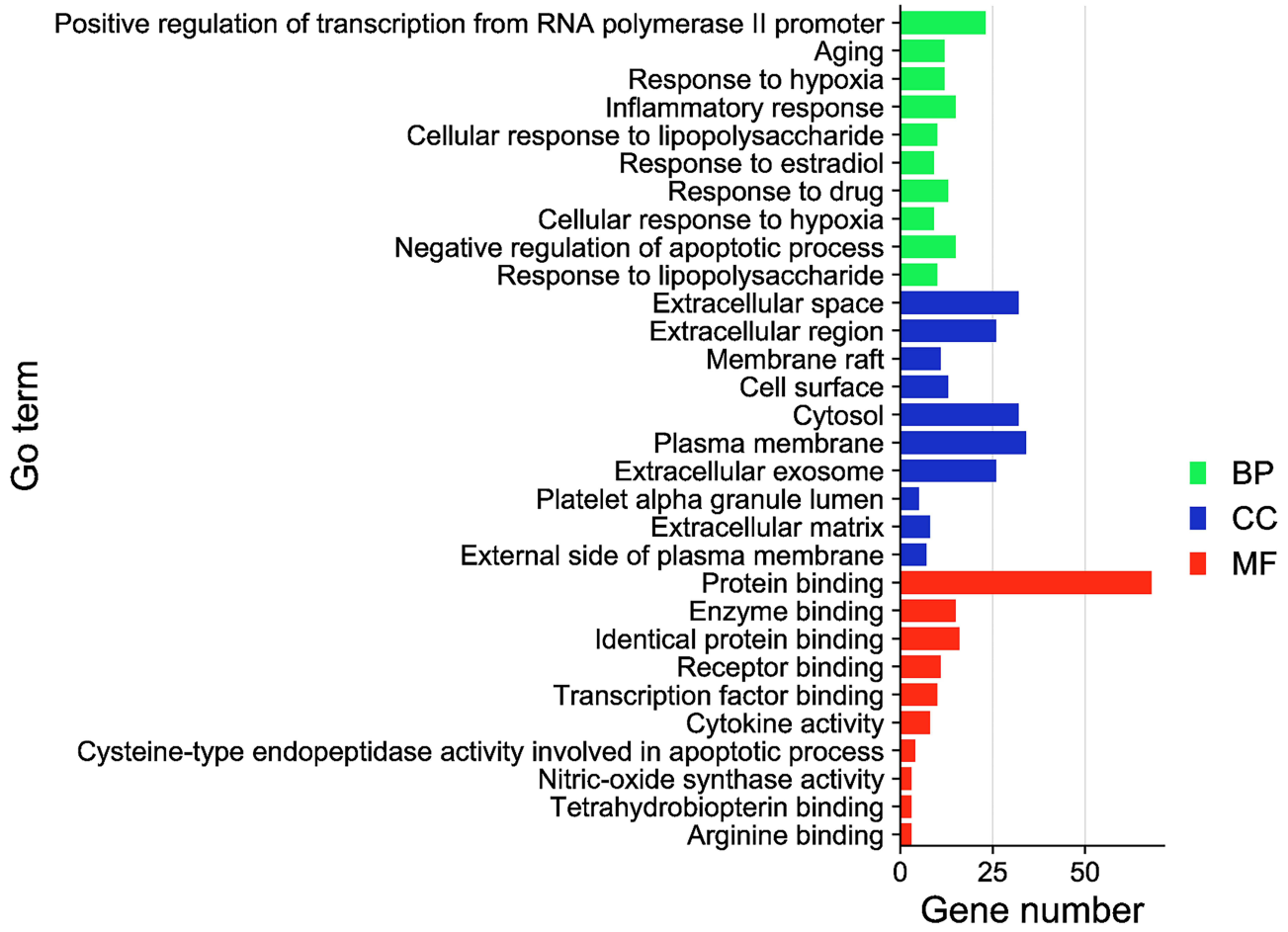

Figure 4 Gene Ontology (GO) enrichment analysis of BYHWD anti-MI/RI targets. Top 10 enriched terms in biological processes (BP), cellular components (CC), and molecular functions (MF).

Table 4 Top 10 Items of Gene Ontology (GO) Enrichment Analysis

GO Items	ID	Description	P value	Gene Number
Biological process	GO:0045944	Positive regulation of transcription from RNA polymerase II promoter	1.15E-10	23
Biological process	GO:0007568	Aging	1.44E-10	12
Biological process	GO:0001666	Response to hypoxia	2.26E-10	12
Biological process	GO:0006954	Inflammatory response	9.36E-10	15
Biological process	GO:0071222	Cellular response to lipopolysaccharide	1.57E-09	10
Biological process	GO:0032355	Response to estradiol	6.12E-09	9
Biological process	GO:0042493	Response to drug	8.04E-09	13
Biological process	GO:0071456	Cellular response to hypoxia	9.38E-09	9
Biological process	GO:0043066	Negative regulation of apoptotic process	9.73E-09	15
Biological process	GO:0032496	Response to lipopolysaccharide	4.17E-08	10
Cellular component	GO:0005615	Extracellular space	1.62E-16	32
Cellular component	GO:0005576	Extracellular region	1.86E-09	26
Cellular component	GO:0045121	Membrane raft	1.05E-08	11
Cellular component	GO:0009986	Cell surface	1.74E-06	13
Cellular component	GO:0005829	Cytosol	1.80E-06	32
Cellular component	GO:0005886	Plasma membrane	2.24E-05	34
Cellular component	GO:0070062	Extracellular exosome	7.01E-05	26
Cellular component	GO:0031093	Platelet alpha granule lumen	7.30E-05	5
Cellular component	GO:0031012	Extracellular matrix	1.97E-04	8
Cellular component	GO:0009897	External side of plasma membrane	2.27E-04	7
Molecular function	GO:0005515	Protein binding	1.06E-12	68
Molecular function	GO:0019899	Enzyme binding	1.61E-10	15
Molecular function	GO:0042802	Identical protein binding	7.00E-07	16
Molecular function	GO:0005102	Receptor binding	3.08E-06	11
Molecular function	GO:0008134	Transcription factor binding	4.04E-06	10
Molecular function	GO:0005125	Cytokine activity	1.19E-05	8
Molecular function	GO:0097153	Cysteine-type endopeptidase activity involved in apoptotic process	2.24E-05	4
Molecular function	GO:0004517	Nitric-oxide synthase activity	5.67E-05	3
Molecular function	GO:0034617	Tetrahydrobiopterin binding	1.13E-04	3
Molecular function	GO:0034618	Arginine binding	3.92E-04	3

signaling pathway displaying the highest centrality, followed by the HIF-1, PI3K/AKT, p53, Toll-like receptor, FoxO, and MAPK signaling pathways (Figure 7).

Molecular Docking Verification

Among the 95 active compounds, six (*quercetin, kaempferol, baicalein, stigmasterol, baicalin*, and *beta-sitosterol*) exhibited the highest degree centralities, prompting us to perform molecular docking with the top 10 hub proteins. The heatmap in Figure 8 displays the binding affinities between these compounds and the hub proteins. The binding affinities range from −5.0 to −10 kcal/mol, with darker colors indicating stronger binding. The results show that *quercetin* and *kaempferol* exhibited the strongest binding affinities with key hub proteins such as AKT1 and TNF, followed by *baicalein, stigmasterol, baicalin*, and *beta-sitosterol*. These findings suggest that the active compounds in BYHWD have potential interactions with the identified hub proteins, which could contribute to the therapeutic effects of BYHWD in MI/RI.

In Figure 9, molecular docking reveals key interactions between BYHWD compounds and target proteins. *Quercetin* binds strongly to AKT1, with hydrogen bonds to THR-211 and LYS-179, and hydrophobic interactions with TYR-229 and MET-227. *Kaempferol* also interacts with AKT1 through hydrogen bonds with GLU-228 and LYS-179, and hydrophobic interactions with ALA-177 and LYS-179. *Beta-sitosterol* binds moderately to IL10, interacting with LEU-94, LEU-98, and MET-77 via hydrophobic forces, suggesting its role in inflammation regulation. *Stigmasterol*

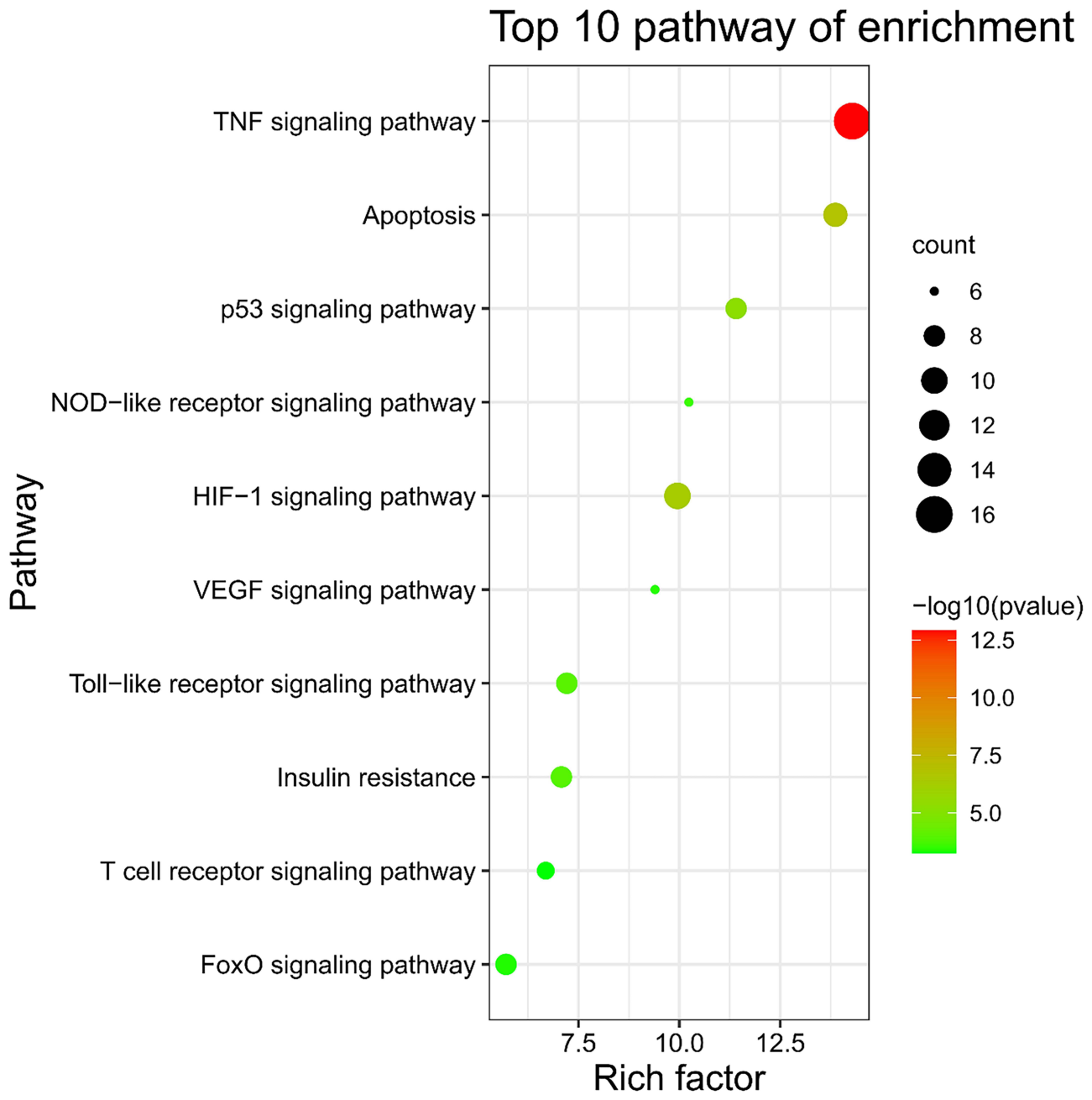

Figure 5 Kyoto Encyclopedia of Genes and Genomes (KEGG) pathway enrichment analysis of myocardial ischemia/reperfusion injury (MI/RI)-related targets. Top 10 pathways ranked by −log10 (P value) and number of involved genes.

interacts with IL10 via both hydrophobic interactions with VAL-124 and PHE-128, and hydrogen bonds with GLU-142. *Baicalein* and *Baicalin* both show strong binding to MMP9, forming hydrogen bonds with key residues (PRO-415, GLU-397, PRO-421, GLY-186, THR-423) and hydrophobic interactions with PHE-145, VAL-398, and MET-422. These interactions suggest that these compounds may modulate their respective pathways to exert therapeutic effects in MI/RI.

BYHWD Reduces Myocardial Infarction Size and Restores Tissue Morphology

TTC staining demonstrated that myocardial tissue in the sham group exhibited consistent red coloration, with minimal evidence of infarction. In contrast, in the MI/RI group, significant infarct size increase was observed, with pale and infarcted walls. Notably, BYHWD treatment reduced infarct size compared to the MI/RI group (Figure 10). HE staining

Table 5 The Enriched 25 Potential Related Pathways for MI/RI

ID	Description	P value	Gene Number
hsa04668	TNF signaling pathway	1.23E-13	16
hsa04210	Apoptosis	1.87E-07	9
hsa04066	HIF-1 signaling pathway	5.02E-07	10
hsa04115	p53 signaling pathway	4.91E-06	8
hsa04620	Toll-like receptor signaling pathway	1.00E-04	8
hsa04931	Insulin resistance	1.13E-04	8
hsa04621	NOD-like receptor signaling pathway	2.58E-04	6
hsa04370	VEGF signaling pathway	3.86E-04	6
hsa04068	FoxO signaling pathway	4.29E-04	8
hsa04660	T cell receptor signaling pathway	5.42E-04	7
hsa04920	Adipocytokine signaling pathway	7.31E-04	6
hsa04919	Thyroid hormone signaling pathway	0.001133136	7
hsa04071	Sphingolipid signaling pathway	0.001412765	7
hsa04064	NF-kappa B signaling pathway	0.001948557	6
hsa04024	cAMP signaling pathway	0.004120887	8
hsa03320	PPAR signaling pathway	0.004895764	5
hsa04622	RIG-I-like receptor signaling pathway	0.005722587	5
hsa04917	Prolactin signaling pathway	0.006017675	5
hsa04151	PI3K-Akt signaling pathway	0.008604042	10
hsa04010	MAPK signaling pathway	0.015008212	8
hsa04915	Estrogen signaling pathway	0.018804544	5
hsa04022	cGMP-PKG signaling pathway	0.023160865	6
hsa04664	Fc epsilon RI signaling pathway	0.032762094	4
hsa04722	Neurotrophin signaling pathway	0.034964361	5
hsa04020	Calcium signaling pathway	0.036944848	6

Abbreviations: MI/RI, myocardial ischemia-reperfusion injury; TNF, tumor necrosis factor; HIF-1, Hypoxia-inducible factor-1; NOD, Nucleotide oligomerization domain; VEGF, vascular endothelial growth factor; FoxO, Forkhead box O; NF-kappa B, nuclear factor kappa-B; cAMP, Cyclic adenosine monophosphate; PPAR, Peroxisome proliferator-activated receptor; RIG-I, Retinoic acid-inducible gene I; PI3K-Akt, Phosphatidylinositol 3-kinase-Protein Kinase B; MAPK, mitogen-activated protein kinase; cGMP-PKG, cyclic guanosine monophosphate-protein kinase G.

showed that myocardial fibers in the sham group were regularly arranged with uniform staining and no obvious signs of tissue damage. In contrast, the MI/RI group showed disordered myocardial fibers, with marked swelling, necrosis, degeneration, and extensive inflammatory cell infiltration in the interstitial spaces. However, BYHWD treatment improved myocardial structure, showing more organized fibers, reduced swelling, and less inflammatory infiltration (Figure 10).

Regulates Protein Expression in MI/RI

Western blot analysis showed significant reductions in ICAM1, VCAM1, and MMP9 expression in BYHWD-treated groups compared to the MI/RI model group. Moreover, BYHWD upregulated phosphorylated AKT1 (*p*-AKT1) levels (Figure 11).

Anti-Inflammatory Effects of BYHWD

ELISA results indicated that BYHWD significantly decreased pro-inflammatory cytokines IL-6 and TNF-α, while increasing anti-inflammatory IL-10 levels (Figure 12), highlighting its anti-inflammatory potential in MI/RI.

Discussion

MI/RI is one of the primary causes of mortality in patients with ischemic heart disease and significantly impacts the outcomes of those with this condition. As such, while the pathogenesis of MI/RI is well-understood, developing safe and

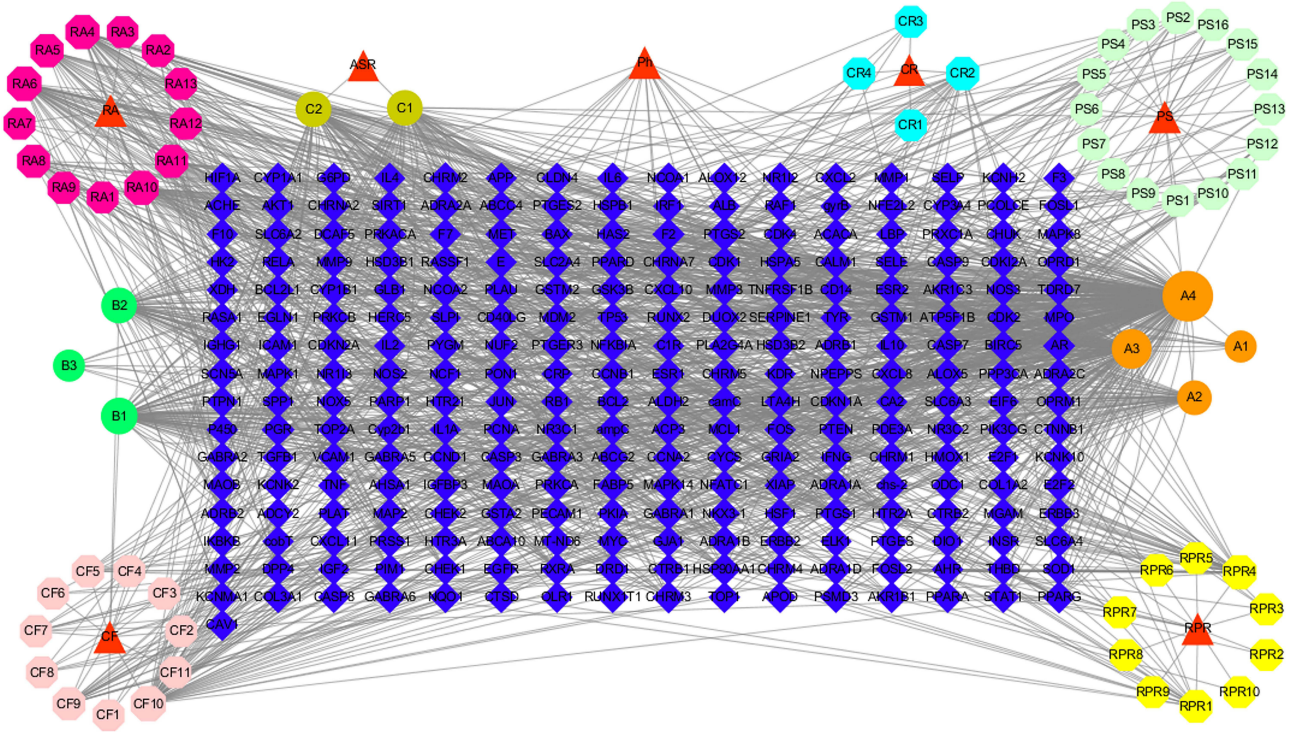

Figure 6 The red triangle represents the herbs contained in BuYang HuanWu Decoction (BYHWD); the blue diamond represents the potential therapeutic targets for BYHWD anti-myocardial ischemia/reperfusion injury (MI/RI); the yellow octagon represents the active compounds contained in *Chi shao* (RPR); the light blue octagon represents the active compounds contained in *Chuang xiong* (CR); the pink octagon represents the active compounds contained in *Hong hua* (CF); the purple octagon represents the active compounds contained in *Huang qi* (RA); the green octagon represents the active compounds contained in *Tao ren* (PS); the ellipse represents the common active compounds of the herb.

effective treatments remains a major challenge due to the limited efficacy of current therapeutic options. These treatments fail to adequately address the underlying mechanisms of ischemic and reperfusion injury, highlighting the need for more effective therapies. This study elucidated the molecular mechanisms by which BYHWD provides cardioprotection against MI/RI using a network pharmacology approach. Specifically, we identified 95 active compounds in BYHWD that influence various biological processes associated with MI/RI, modulating myocardial ischemia outcomes through pathways such as TNF signaling pathway, apoptosis, and p53 signaling pathway.

Quercetin, a flavonoid found in several herbs, is one of the primary cardioprotective components in the compound-target network. Research has demonstrated that *quercetin* exerts cardioprotective effects on isolated heart tissues affected by MI/RI injury via the HMGB1/TLR/NF-κB pathway.[47] Additionally, Zhang et al reported that *quercetin* reduces oxidative stress damage by blocking NADPH oxidase. Its anti-inflammatory and anti-apoptotic properties mitigate inflammatory responses and prevent myocardial cell apoptosis.[48] Furthermore, Tang et al showed that *quercetin* enhances cardiomyocyte survival during MI/RI by regulating the SIRT1/PGC-1α signaling pathway.[49]

Kaempferol, another prominent flavonoid, is well-recognized for its antioxidant and anti-inflammatory properties.[50] Dong et al demonstrated that *kaempferol* alleviates oxidative stress and inflammatory responses, reducing myocardial infarct size in MI/RI by inhibiting the Nrf2 and cleaved caspase-3 signaling pathways.[51] Additionally, Zhou et al found that *kaempferol* provides cardiac protection during MI/RI by inhibiting the GSK-3β pathway.[52] These findings suggest that *kaempferol* holds significant potential as a treatment for MI/RI.

Baicalein and *baicalin*, major constituents of *Carthami Flos* and *Radix Paeoniae Rubra*, exhibit a range of beneficial properties, including antiviral, antioxidant, anticancer, anti-apoptotic, and anti-inflammatory effects.[53,54] Song et al showed that *baicalein* reduces myocardial infarction size and alleviates MI/RI by activating the ERK1/2 and AKT pathways.[55] Similarly, Luan et al reported that *baicalin* can alleviate inflammation reaction and apoptosis during MI/RI by regulating the Akt/NF-κB pathway.[56]

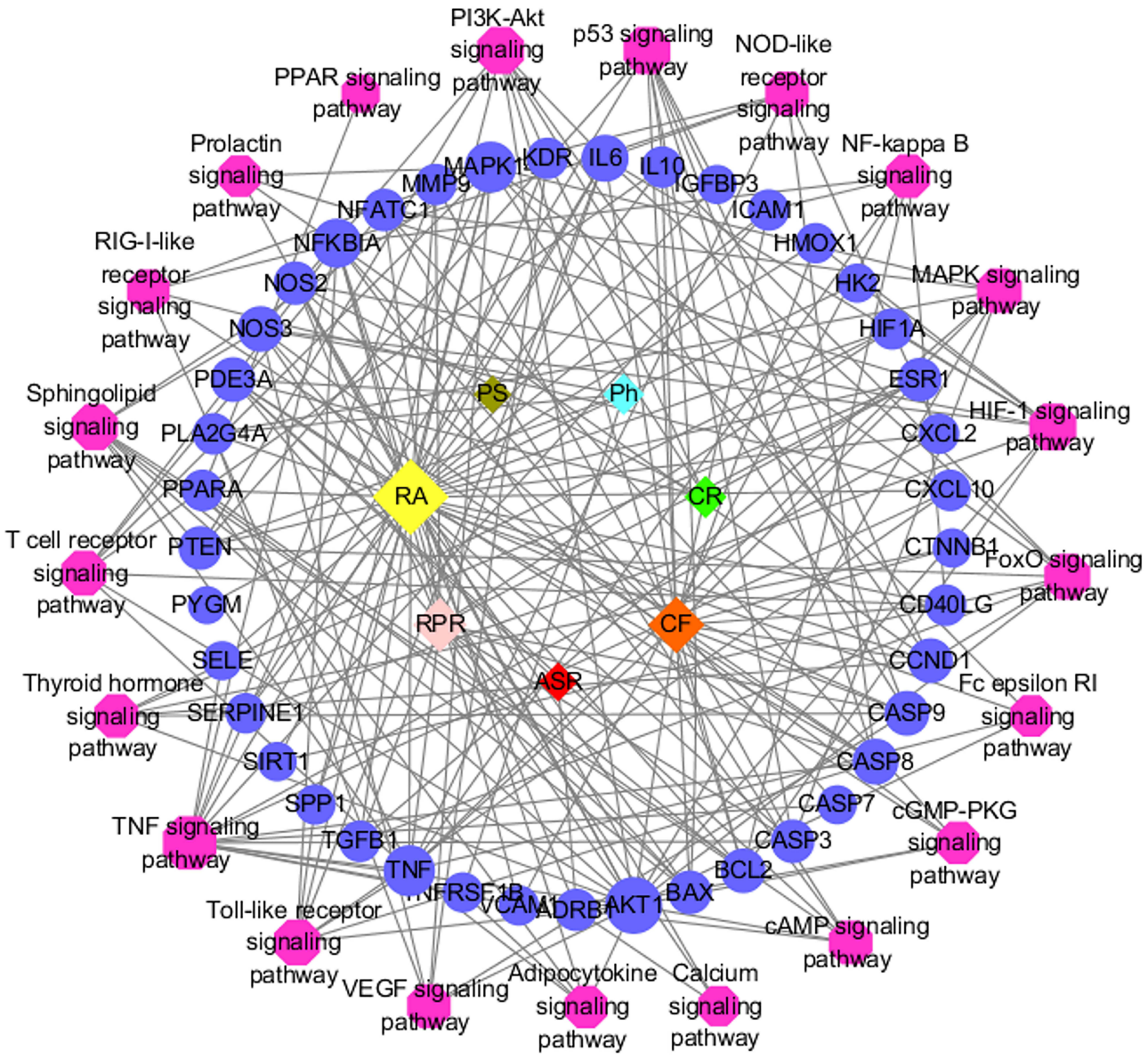

Figure 7 Herb-target-pathway network. The purple circles stand for 25 myocardial ischemia/reperfusion injury (MI/RI)-related pathways and the red, yellow, green, dark green, light blue, pink, and Orange diamond stand for compounds of *Angelicae Sinensis Radix, Radix Astragali, Chuanxiong Rhizoma, Persicae Semen, Pheretima, Radix Paeoniae Rubra*, and *Carthami Flos*, respectively. Besides, blue circles stand for genes related to BuYang HuanWu Decoction (BYHWD).

Luteolin, another component of *Carthami Flos*, has been shown to reduce LDH and CK-MB levels, as well as diminish leukocyte infiltration and cytokine levels in MI/RI rats by modulating the Sirt1/NF-κB pathway.[57] In vivo studies further demonstrated that *luteolin* decreases infarct size, suggesting that *luteolin* may protect the heart by upregulating SERCA2a and Sp1.[58]

Persicae Semen, Radix Paeoniae Rubra, Carthami Flos, and *Angelicae Sinensis Radix* all contain *beta-sitosterol* and *stigmasterol*, which are increasingly recognized for their beneficial roles in cardiovascular diseases. Lin et al showed that *beta-sitosterol* can reduce myocardial MI/RI injury in vivo by influencing the PPARγ/NF-κB signaling pathway.[59] These findings suggest that BYHWD may provide cardioprotection through various components, targets, and pathways.

PPI analysis identified IL6, TNF, AKT1, ICAM1, IL10, MMP-9, VCAM1, NOS3, ALB, and CRP as the top ten targets with the highest MCC scores. Additionally, pathway enrichment analysis revealed that the primary pathways involved were TNF signaling, apoptosis, p53 signaling, and VEGF signaling. IL6, TNF, and CRP are well-known inflammatory cytokines that trigger inflammatory responses, exacerbating myocardial damage during ischemia/

https://doi.org/10.2147/JIR.S512050

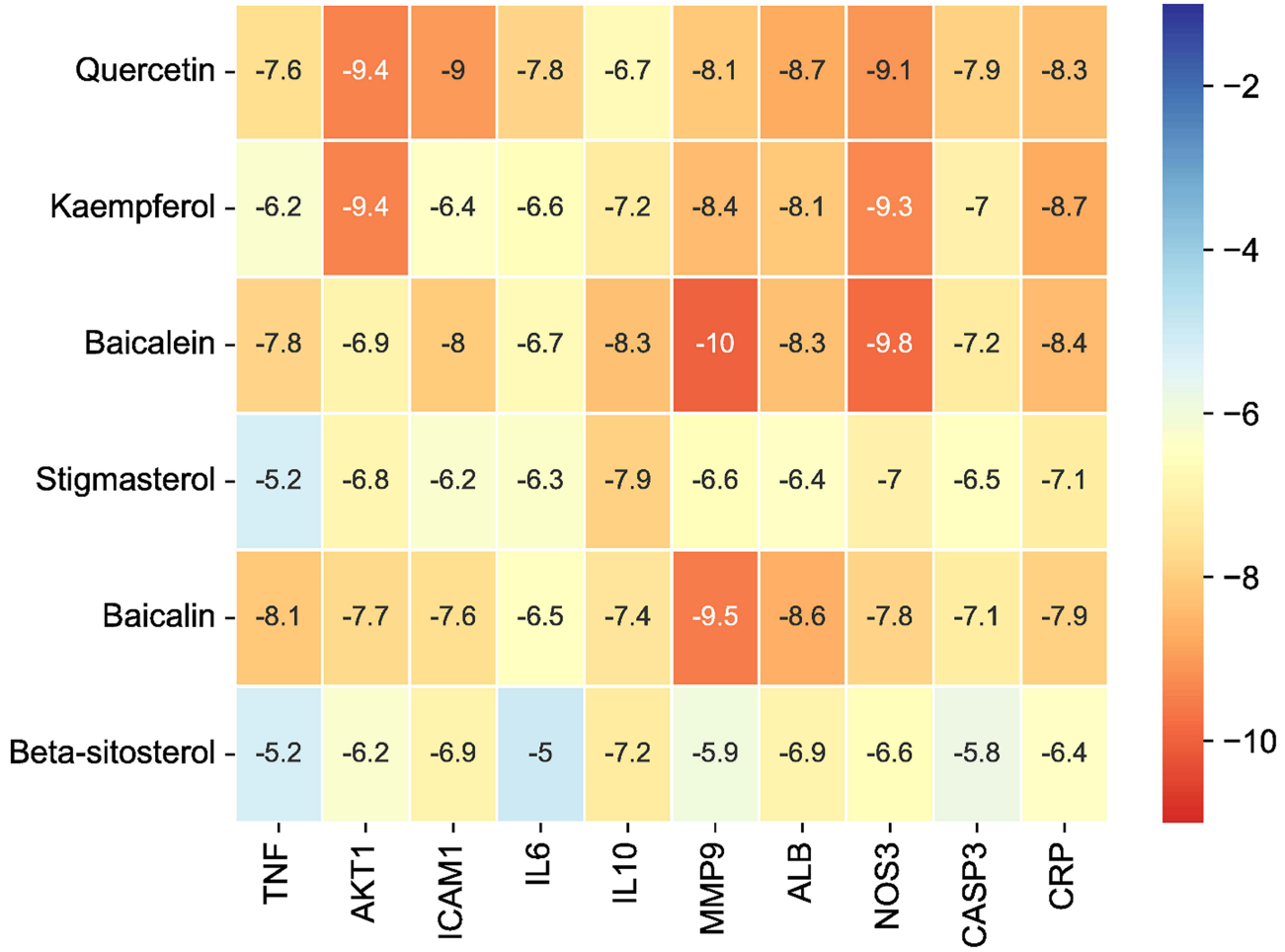

Figure 8 Heatmap of the scores of molecular docking in this study.

reperfusion injury (MI/RI). In contrast, IL-10, a significant anti-inflammatory cytokine, is associated with reduced myocardial damage.[60] In this study, BYHWD treatment significantly reduced pro-inflammatory cytokines IL-6 and TNF-α, while increasing anti-inflammatory IL-10 levels. These findings suggest that BYHWD may counteract inflammation and mitigate MI/RI through its modulation of key inflammatory cytokines.

ICAM1 is an adhesion molecule that mediates adhesion reactions and plays an important role in vascular endothelial dysfunction. ICAM-1 can induce circulating leukocytes to adhere to the endothelium and migrate to the vascular intima, aggravating the inflammatory response and leading to myocardial injury during MI/RI.[61] ICAM-1 and VCAM-1, as key adhesion molecules, play a critical role in the migration of leukocytes and the amplification of inflammatory responses during MIRI, contributing to endothelial dysfunction and tissue damage.[62] MMP-9 is the most important enzyme of matrix metalloproteinase (MMPs). Increased MMP-9 expression is associated with inflammation, microvascular synthesis, extracellular matrix degradation and synthesis, and cardiac dysfunction during MI/RI.[63] AKT1 is a serine/threonine-protein kinase (AKT1, AKT2, and AKT3) that plays a crucial role in major cellular functions, including cell growth, the cell cycle, glucose metabolism, transcription, protein synthesis, and angiogenesis.[64] AKT1 plays a key role in angiogenesis, particularly the activation of phosphorylated AKT1 (*p*-AKT1), is well established as a key mediator of cellular survival and anti-inflammatory responses. Activation of *p*-AKT1 can mitigate apoptotic pathways, reduce oxidative stress, and enhance endothelial barrier function, collectively protecting cardiac tissues from reperfusion injury.[65] Our study found that BYHWD significantly downregulated the expression of ICAM-1, VCAM-1, and MMP-9, while upregulating the expression of p-AKT1 compared to the MI/RI group. Furthermore, significant binding affinities were

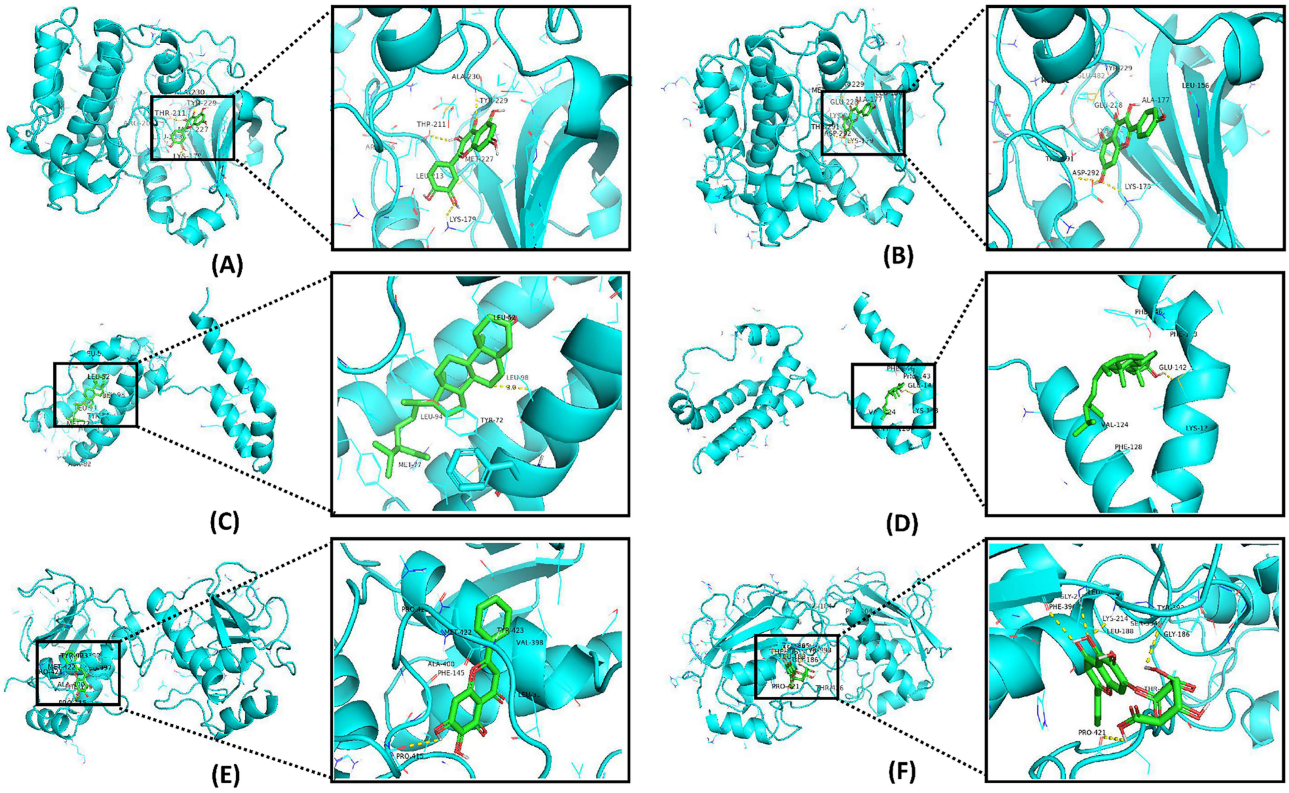

Figure 9 Results of molecular docking between hub genes and key active compounds. (**A**) Protein Kinase B alpha (AKT1) with *quercetin*, (**B**) AKT1 with *kaempferol*, (**C**) Interleukin-10 (IL-10) with *beta-sitosterol*, (**D**) IL-10 with *stigmasterol*, (**E**) Matrix metalloproteinase-9 (MMP9) with *baicalein*, (**F**) MMP9 with *baicalin*. Yellow lines represent hydrogen bonds between the protein and the ligand. Green lines indicate hydrophobic interactions. Red lines show electrostatic interactions or ionic bonds. The stick model represents the ligand, while the ribbon model represents the protein structure. The residue labels indicate key amino acids involved in the interactions.

observed between hub genes and key compounds of BYHWD, indicating potential interactions. These findings underscore the therapeutic potential of BYHWD in attenuating MIRI through multi-target and multi-pathway effects.

However, this study had several limitations. First, the potential components of BYHWD identified through database mining rely heavily on previously published data. It is plausible that this formula contains additional, as-yet-undiscovered compounds, which could be identified using more advanced network pharmacology methodologies, such as multilevel network analysis, GWAS-based network pharmacology, and global network reconstruction and drug repurposing. These methodologies combine various layers of data and offer a more comprehensive approach to identifying critical compounds and their underlying mechanisms. Second, the predicted targets and pathways were derived from existing databases and literature, which may limit the discovery of novel mechanisms underlying MIRI pathogenesis and the pharmacological actions of BYHWD. Third, future research should consider including standardized drugs or interventions as comparisons in in vivo preclinical studies to provide a more robust evaluation of BYHWD's therapeutic effects. Finally, we did not evaluate the dose-dependent effects of BYHWD on MI/RI, which could further elucidate the relationship between dosage and therapeutic efficacy. We will further elaborate on the dose-dependent effects of BYHWD, as well as the potential long-term impacts of its usage, based on the current data and future directions for research. This will provide a more comprehensive understanding of the therapeutic potential and safety profile of BYHWD. Future research should focus on comprehensive in vivo studies and well-designed clinical trials to validate the protective effects and optimal dosing of BYHWD in MI/RI.

Conclusions

We explored the mechanisms underlying the cardioprotective effects of BYHWD in MI/RI through a network pharmacology approach and in vivo validation. Key therapeutic targets identified in this study include AKT1, TNF, IL6, MMP9,

 https://doi.org/10.2147/JIR.S512050

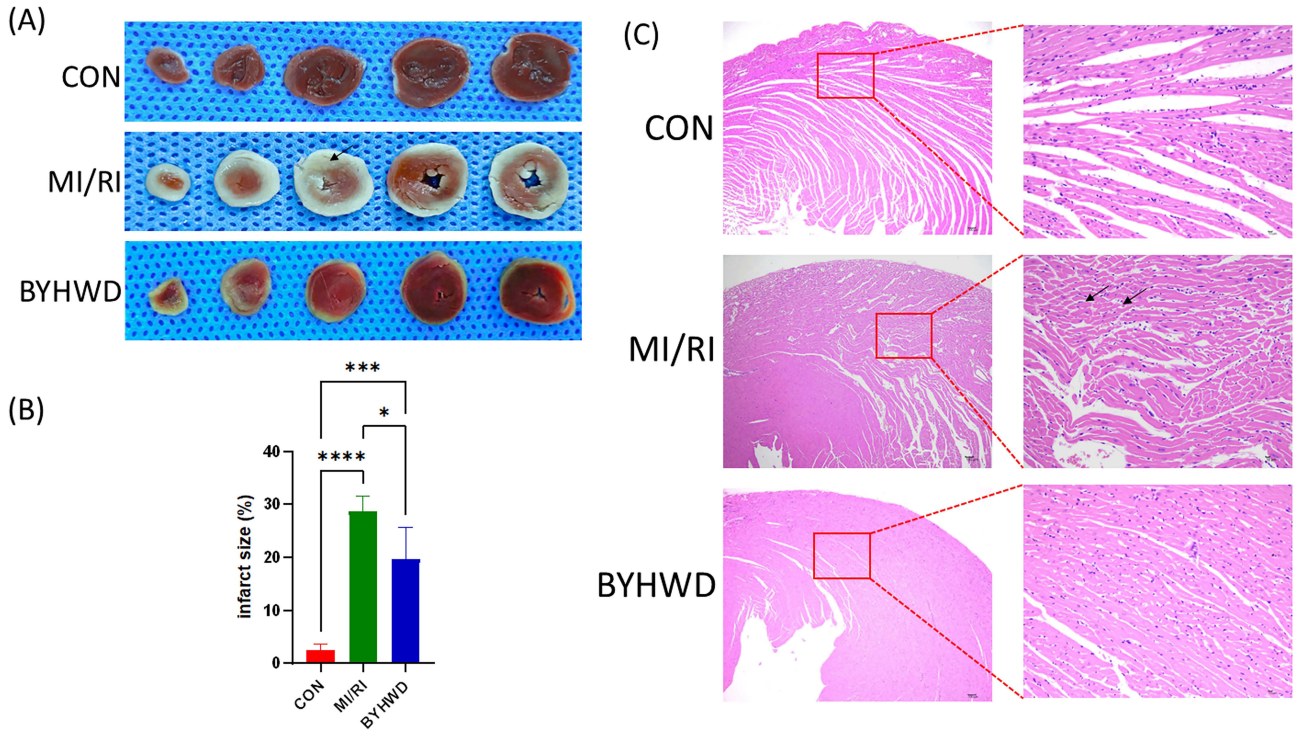

Figure 10 Effect of BuYang HuanWu Decoction (BYHWD) on myocardial infarction size and myocardial tissue pathological morphology. (**A** and **B**) Representative images of myocardial infarct size in each group, assessed using triphenyltetrazolium chloride (TTC) staining. Recombinant Human Glutathione Peroxidase 4 (rhGPx4) prevents pathological damage of myocardial ischemia. The black arrow indicates the location of myocardial ischemia/reperfusion injury (MI/RI). (**C**) Representative hematoxylin-eosin (HE) staining images showing myocardial tissue morphology in each group. The black arrows indicate cardiomyocyte necrosis, edema, and inflammatory cell infiltration. *p < 0.05, **p < 0.01, ***p < 0.001, ****p < 0.0001; sample size, n = 4.

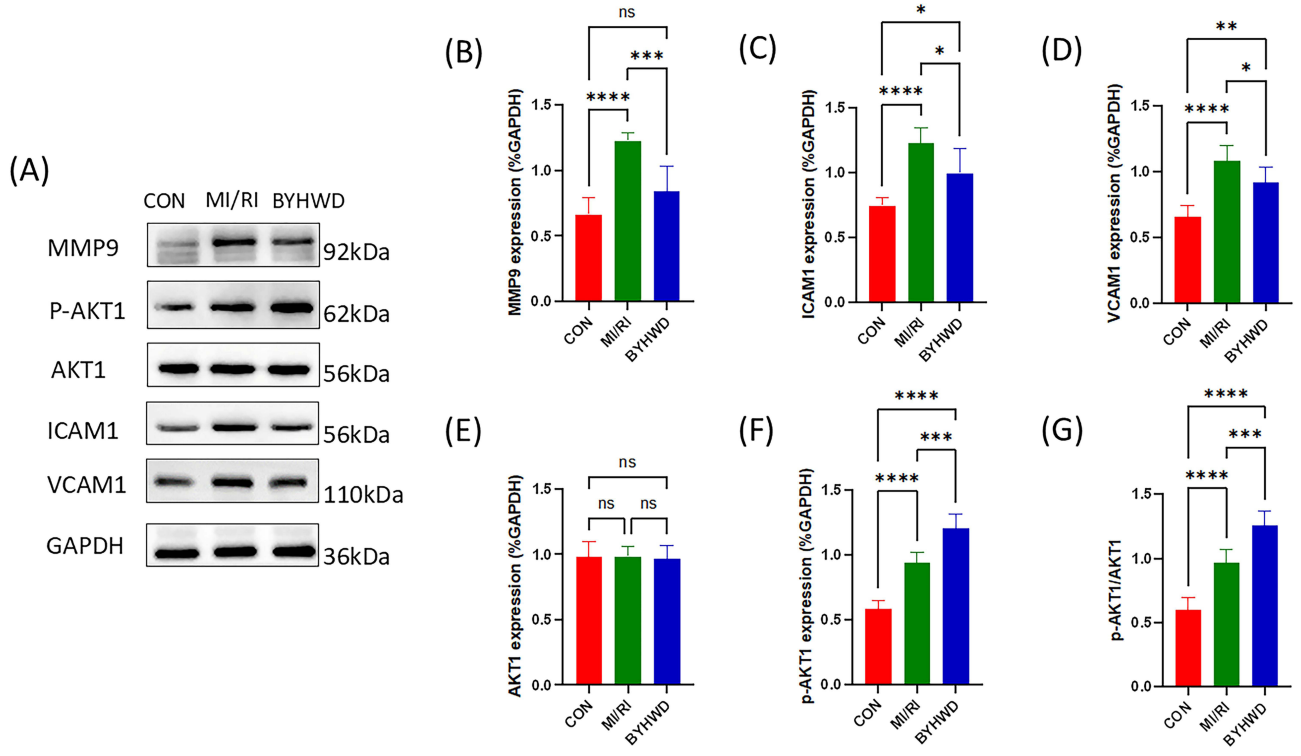

Figure 11 Effect of BuYang HuanWu Decoction (BYHWD) on protein expression of hub genes. (**A**–**G**) Western blot analysis for the protein expression levels of Intercellular Adhesion Molecule 1 (ICAM-1), Vascular Cell Adhesion Molecule 1 (VCAM-1), Matrix Metalloproteinase-9 (MMP-9), and Protein Kinase B alpha (AKT1) / Phosphorylated AKT1 (p-AKT1) in each group. *p < 0.05, **p < 0.01, ***p < 0.001, ****p < 0.0001; ns = not significant, sample size, n = 6.

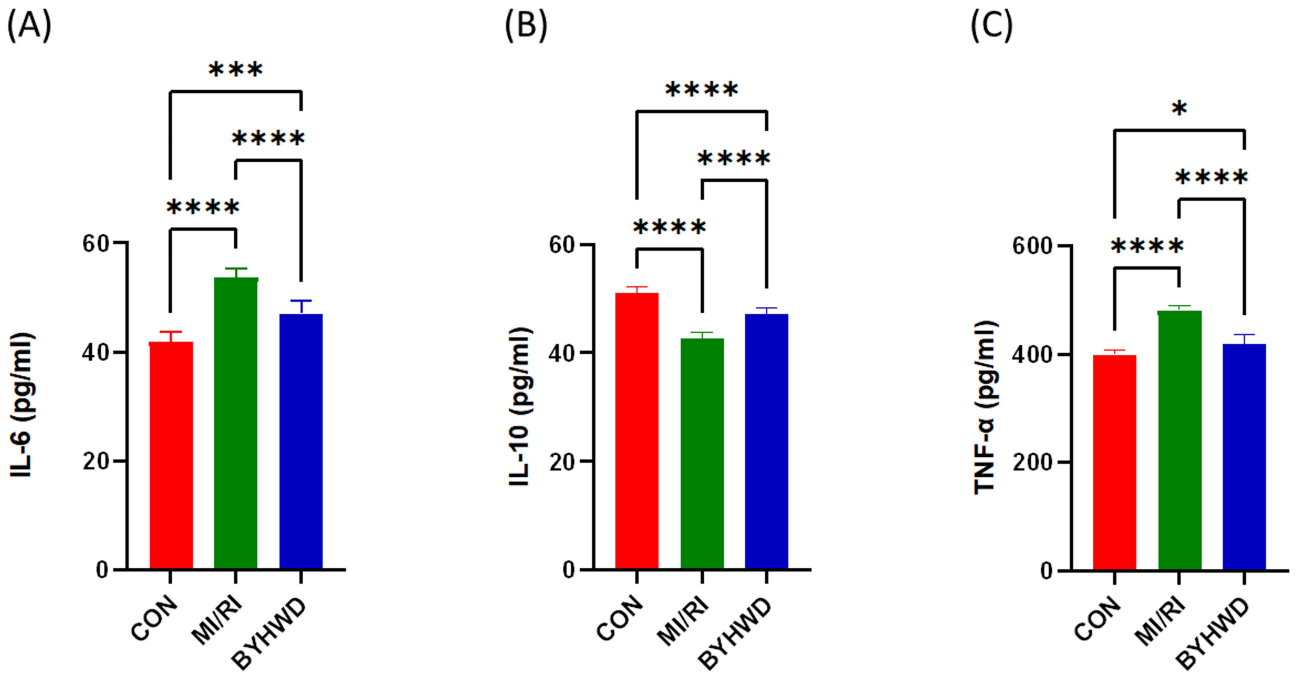

Figure 12 Effect of BuYang HuanWu Decoction (BYHWD) on inflammatory cytokine expression (**A**–**C**) Enzyme-Linked Immunosorbent Assay (ELISA) analysis showing the expression levels of inflammatory cytokines Tumor Necrosis Factor-alpha (TNF-α), Interleukin-6 (IL-6), and Interleukin-10 (IL-10) in each group. * $p<0.05$, ** $p<0.01$, *** $p<0.001$, **** $p<0.0001$, n=6.

IL10, ICAM1, ALB, NOS3, CASP3, and CRP. The main bioactive compounds in BYHWD, *quercetin, kaempferol, baicalein, stigmasterol, baicalin*, and *beta-sitosterol* were shown to play key roles in combating MI/RI. Enrichment analysis revealed several key pathways involved, including TNF signaling, apoptosis, and p53 signaling. Molecular docking studies demonstrated that these active compounds effectively bind to the identified key targets. Furthermore, in vivo experiments demonstrated that BYHWD significantly reduced myocardial infarct size, suppressed the expression of pro-inflammatory cytokines IL-6 and TNF-α, decreased the levels of ICAM1, VCAM1, and MMP9 proteins, and enhanced anti-inflammatory cytokine IL-10 and phosphorylated AKT1 (p-AKT1) protein expression. These findings reveal the multi-component, multi-target, and multi-pathway mechanisms by which BYHWD exerts cardioprotective effects against MI/RI.

Abbreviations

MI/RI, Myocardial ischemial reperfusion injury; BYHWD, Buyang Huanwu decoction; AMI, Acute myocardial infarction (AMI); PCI, percutaneous coronary intervention; TCM, traditional Chinese medicine; GO, Gene Ontology; KEGG, Kyoto Encyclopedia of Genes and Genomes; PPI, protein-protein interact; ADME, absorption, distribution, metabolism, and excretion; OB, oral bioavailability; DL, drug-likeness; SDF, specific-pathogen-free; SD, Sprague-Dawley; LAD, left anterior descending; BP, biological process; CC, cellular component; MF, molecular function; TTC, triphenyltetrazolium chloride; HE, Hematoxylin and eosin; HMGB1, High Mobility Group Box 1; TLR, Toll-Like Receptor; NF-κB, Nuclear Factor-kappa B; SIRT1, Sirtuin 1; PGC-1α, Peroxisome Proliferator-Activated Receptor Gamma Coactivator 1 Alpha; GSK-3β, Glycogen Synthase Kinase 3 Beta; ERK1/2, Extracellular Signal-Regulated Kinase 1/2; AKT, Protein Kinase B; PPARγ, Peroxisome Proliferator-Activated Receptor Gamma; VEGF, Vascular Endothelial Growth Factor.

Ethics and Animal Welfare

The animal study protocol was approved by the Animal Ethics Committee of Guizhou Medical University on the Use and Care of Animals of Guizhou Medical University (protocol code 2305219) for studies involving animals. All procedures in this study were conducted in accordance with the Animal Care Welfare Committee of Guizhou Medical University

https://doi.org/10.2147/JIR.S512050

(Guiyang, China). This study also adhered to the National Institutes of Health guidelines outlined in their "Guide for the Care and Use of Laboratory Animals".

Author Contributions

All authors made a significant contribution to the work reported, whether that is in the conception, study design, execution, acquisition of data, analysis and interpretation, or in all these areas; took part in drafting, revising or critically reviewing the article; gave final approval of the version to be published; have agreed on the journal to which the article has been submitted; and agree to be accountable for all aspects of the work.

Funding

This work was supported by the National Natural Science Foundation of China (No. 82160951), the Cultivate Project 2021 for National Natural Science Foundation of China, the Affiliated Hospital of Guizhou Medical University (gyfynsfc-2021-35), Guiyang Gui'an Science and Technology Talent Training Program (zhukehe [2024]2-27), Traditional Chinese Medicine Project of Guizhou (QZYY-2019-013), and Key Laboratory of Anesthesia and Pain Research of Guizhou Medical University ([2024]fy003).

Disclosure

Yushan Luo, Wen Hu, Ziyue Li and Xiaoyuan Zhang contributed equally and share co-first authors for this study. The authors declare no conflicts of interest.

References

1. Benjamin EJ, Blaha MJ, Chiuve SE, et al. Heart disease and stroke statistics-2017 update: a report from the American Heart Association. *Circulation*. 2017;135(10):e146–e603. doi:10.1161/cir.0000000000000485
2. Meng ZQ, Wu JR, Zhu YL, et al. Revealing the common mechanisms of scutellarin in angina pectoris and ischemic stroke treatment via a network pharmacology approach. *Chin J Integr Med*. 2021;27(1):62–69. doi:10.1007/s11655-020-2716-4
3. Reed GW, Rossi JE, Cannon CP. Acute myocardial infarction. *Lancet*. 2017;389(10065):197–210. doi:10.1016/s0140-6736(16)30677-8
4. Yang CF. Clinical manifestations and basic mechanisms of myocardial ischemia/reperfusion injury. *Tzu Chi Med J*. 2018;30(4):209–215. doi:10.4103/tcmj.tcmj_33_18
5. Bellanti F. Hypoxia-inducible factor-1 in myocardial ischaemia/reperfusion injury. *Acta Physiol*. 2017;221(2):93–94. doi:10.1111/apha.12903
6. Yang J, Xiang Z, Zhang J, et al. miR-24 alleviates MI/RI by blocking the S100A8/TLR4/MyD88/NF-kB pathway. *J Cardiovasc Pharmacol*. 2021;78(6):847–857. doi:10.1097/fjc.0000000000001139
7. Zhou P, Zhang Y, Xu K, et al. Uncoupling protein 2 alleviates myocardial ischemia/reperfusion injury by inhibiting cardiomyocyte ferroptosis. *J Vasc Res*. 2024;61(3):109–121. doi:10.1159/000537925
8. Lv L, Kong Q, Li Z, et al. Honokiol provides cardioprotection from Myocardial Ischemia/Reperfusion Injury (MI/RI) by inhibiting mitochondrial apoptosis via the PI3K/AKT signaling pathway. *Cardiovasc Ther*. 2022;2022:1001692. doi:10.1155/2022/1001692
9. Davidson SM, Ferdinandy P, Andreadou I, et al. Multitarget strategies to reduce myocardial ischemia/reperfusion injury: JACC review topic of the week. *J Am Coll Cardiol*. 2019;73(1):89–99. doi:10.1016/j.jacc.2018.09.086
10. Long L, Yu Z, Chen S, et al. Pretreatment of Huoxue Jiedu formula ameliorates myocardial ischaemia/reperfusion injury by decreasing autophagy via activation of the PI3K/AKT/mTOR pathway. *Front Pharmacol*. 2021;12:608790. doi:10.3389/fphar.2021.608790
11. Zhang Z, Qin X, Wang Z, et al. Oxymatrine pretreatment protects H9c2 cardiomyocytes from hypoxia/reoxygenation injury by modulating the PI3K/Akt pathway. *Exp Ther Med*. 2021;21(6):556. doi:10.3892/etm.2021.9988
12. Li Q, Yu Z, Xiao D, et al. Baicalein inhibits mitochondrial apoptosis induced by oxidative stress in cardiomyocytes by stabilizing MARCH5 expression. *J Cell Mol Med*. 2020;24(2):2040–2051. doi:10.1111/jcmm.14903
13. Zhang M, Chai Y, Liu T, Xu N, Yang C. Synergistic effects of Buyang Huanwu decoction and embryonic neural stem cell transplantation on the recovery of neurological function in a rat model of spinal cord injury. *Exp Ther Med*. 2015;9(4):1141–1148. doi:10.3892/etm.2015.2248
14. Lee YS, Woo SC, Kim SY, Park JY. Understanding the multi-herbal composition of Buyang Huanwu Decoction: a review for better clinical use. *J Ethnopharmacol*. 2020;255:112765. doi:10.1016/j.jep.2020.112765
15. Gao Q, Tian D, Han Z, et al. Network pharmacology and molecular docking analysis on molecular targets and mechanisms of buyang Huanwu decoction in the treatment of ischemic stroke. *Evid Based Complement Alternat Med*. 2021;2021:8815447. doi:10.1155/2021/8815447
16. Wang WR, Lin R, Zhang H, et al. The effects of Buyang Huanwu Decoction on hemorheological disorders and energy metabolism in rats with coronary heart disease. *J Ethnopharmacol*. 2011;137(1):214–220. doi:10.1016/j.jep.2011.05.008
17. Zhang H, Wang WR, Lin R, et al. Buyang Huanwu decoction ameliorates coronary heart disease with Qi deficiency and blood stasis syndrome by reducing CRP and CD40 in rats. *J Ethnopharmacol*. 2010;130(1):98–102. doi:10.1016/j.jep.2010.04.017
18. Zhu JZ, Bao XY, Zheng Q, et al. Buyang Huanwu decoction exerts cardioprotective effects through targeting angiogenesis via Caveolin-1/VEGF signaling pathway in mice with acute myocardial infarction. *Oxid Med Cell Longev*. 2019;2019:4275984. doi:10.1155/2019/4275984
19. Wang HW, Liou KT, Wang YH, et al. Deciphering the neuroprotective mechanisms of Bu-yang Huan-wu decoction by an integrative neurofunctional and genomic approach in ischemic stroke mice. *J Ethnopharmacol*. 2011;138(1):22–33. doi:10.1016/j.jep.2011.06.033

20. Chen ZZ, Gong X, Guo Q, Zhao H, Wang L. Bu Yang Huan Wu decoction prevents reperfusion injury following ischemic stroke in rats via inhibition of HIF-1 α, VEGF and promotion β-ENaC expression. *J Ethnopharmacol*. 2019;228:70–81. doi:10.1016/j.jep.2018.09.017
21. Xue B, Ma B, Yao Y, Zhao A, Gao Y, Liu J. BYHW decoction improves cognitive impairments in rats with cerebral microinfarcts via activation of the PKA/CREB pathway. *Oxid Med Cell Longev*. 2022;2022:4455654. doi:10.1155/2022/4455654
22. Mu Q, Liu P, Hu X, Gao H, Zheng X, Huang H. Neuroprotective effects of Buyang Huanwu decoction on cerebral ischemia-induced neuronal damage. *Neural Regen Res*. 2014;9(17):1621–1627. doi:10.4103/1673-5374.141791
23. Liu X, Wu J, Zhang D, et al. Network pharmacology-based approach to investigate the mechanisms of hedyotis diffusa Willd. in the treatment of gastric cancer. *Evid Based Complement Alternat Med*. 2018;2018:7802639. doi:10.1155/2018/7802639
24. Chandran U, Mehendale N, Tillu G, Patwardhan B. Network pharmacology of ayurveda formulation triphala with special reference to anti-cancer property. *Comb Chem High Throughput Screen*. 2015;18(9):846–854. doi:10.2174/1386207318666151019093606
25. Ru J, Li P, Wang J, et al. TCMSP: a database of systems pharmacology for drug discovery from herbal medicines. *J Cheminform*. 2014;6:13. doi:10.1186/1758-2946-6-13
26. Xu HY, Zhang YQ, Liu ZM, et al. ETCM: an encyclopaedia of traditional Chinese medicine. *Nucleic Acids Res*. 2019;47(D1):D976–d982. doi:10.1093/nar/gky987
27. Liu Z, Guo F, Wang Y, et al. BATMAN-TCM: a bioinformatics analysis tool for molecular mechANism of traditional Chinese medicine. *Sci Rep*. 2016;6:21146. doi:10.1038/srep21146
28. Shi XQ, Yue SJ, Tang YP, et al. A network pharmacology approach to investigate the blood enriching mechanism of Danggui buxue Decoction. *J Ethnopharmacol*. 2019;235:227–242. doi:10.1016/j.jep.2019.01.027
29. Tsaioun K, Blaauboer BJ, Hartung T. Evidence-based absorption, distribution, metabolism, excretion (ADME) and its interplay with alternative toxicity methods. *Altex*. 2016;33(4):343–358. doi:10.14573/altex.1610101
30. UniProt Consortium T. UniProt: the universal protein knowledgebase. *Nucleic Acids Res*. 2018;46(5):2699. doi:10.1093/nar/gky092
31. Piñero J, Bravo À, Queralt-Rosinach N, et al. DisGeNET: a comprehensive platform integrating information on human disease-associated genes and variants. *Nucleic Acids Res*. 2017;45(D1):D833–d839. doi:10.1093/nar/gkw943
32. Stelzer G, Rosen N, Plaschkes I, et al. The GeneCards suite: from gene data mining to disease genome sequence analyses. *Curr Protoc Bioinformatics*. 2016;54:1.30.1–1.30.33. doi:10.1002/cpbi.5
33. Keiser MJ, Roth BL, Armbruster BN, Ernsberger P, Irwin JJ, Shoichet BK. Relating protein pharmacology by ligand chemistry. *Nat Biotechnol*. 2007;25(2):197–206. doi:10.1038/nbt1284
34. Davis AP, Grondin CJ, Johnson RJ, et al. Comparative Toxicogenomics Database (CTD): update 2021. *Nucleic Acids Res*. 2021;49(D1):D1138–d1143. doi:10.1093/nar/gkaa891
35. Wang Y, Zhang S, Li F, et al. Therapeutic target database 2020: enriched resource for facilitating research and early development of targeted therapeutics. *Nucleic Acids Res*. 2020;48(D1):D1031–d1041. doi:10.1093/nar/gkz981
36. Zhu J, Yi X, Zhang Y, Pan Z, Zhong L, Huang P. Systems pharmacology-based approach to comparatively study the independent and synergistic mechanisms of danhong injection and naoxintong capsule in ischemic stroke treatment. *Evid Based Complement Alternat Med*. 2019;2019:1056708. doi:10.1155/2019/1056708
37. Rappaport N, Twik M, Plaschkes I, et al. MalaCards: an amalgamated human disease compendium with diverse clinical and genetic annotation and structured search. *Nucleic Acids Res*. 2017;45(D1):D877–d887. doi:10.1093/nar/gkw1012
38. Franceschini A, Szklarczyk D, Frankild S, et al. STRING v9.1: protein-protein interaction networks, with increased coverage and integration. *Nucleic Acids Res*. 2013;41(Database issue):D808–15. doi:10.1093/nar/gks1094
39. Xu T, Ma C, Fan S, et al. Systematic understanding of the mechanism of baicalin against ischemic stroke through a network pharmacology approach. *Evid Based Complement Alternat Med*. 2018;2018:2582843. doi:10.1155/2018/2582843
40. Zhang MM, Wang D, Lu F, et al. Identification of the active substances and mechanisms of ginger for the treatment of colon cancer based on network pharmacology and molecular docking. *BioData Min*. 2021;14(1):1. doi:10.1186/s13040-020-00232-9
41. Trott O, Olson AJ. AutoDock Vina: improving the speed and accuracy of docking with a new scoring function, efficient optimization, and multithreading. *J Comput Chem*. 2010;31(2):455–461. doi:10.1002/jcc.21334
42. Goodsell DS, Dutta S, Zardecki C, Voigt M, Berman HM, Burley SK. The RCSB PDB "Molecule of the Month": inspiring a molecular view of biology. *PLoS Biol*. 2015;13(5):e1002140. doi:10.1371/journal.pbio.1002140
43. Vrontaki E, Melagraki G, Mavromoustakos T, Afantitis A. Searching for anthranilic acid-based thumb pocket 2 hCV NS5B polymerase inhibitors through a combination of molecular docking, 3D-QSAR and virtual screening. *J Enzyme Inhib Med Chem*. 2016;31(1):38–52. doi:10.3109/14756366.2014.1003925
44. Morris GM, Huey R, Lindstrom W, et al. AutoDock4 and AutoDockTools4: automated docking with selective receptor flexibility. *J Comput Chem*. 2009;30(16):2785–2791. doi:10.1002/jcc.21256
45. Gaillard T. Evaluation of AutoDock and AutoDock Vina on the CASF-2013 Benchmark. *J Chem Inf Model*. 2018;58(8):1697–1706. doi:10.1021/acs.jcim.8b00312
46. Cai G, Liu B, Liu W, et al. Buyang Huanwu Decoction can improve recovery of neurological function, reduce infarction volume, stimulate neural proliferation and modulate VEGF and Flk1 expressions in transient focal cerebral ischaemic rat brains. *J Ethnopharmacol*. 2007;113(2):292–299. doi:10.1016/j.jep.2007.06.007
47. Dong LY, Chen F, Xu M, Yao LP, Zhang YJ, Zhuang Y. Quercetin attenuates myocardial ischemia-reperfusion injury via downregulation of the HMGB1-TLR4-NF-κB signaling pathway. *Am J Transl Res*. 2018;10(5):1273–1283.
48. Zhang YM, Zhang ZY, Wang RX. Protective mechanisms of quercetin against myocardial ischemia reperfusion injury. *Front Physiol*. 2020;11:956. doi:10.3389/fphys.2020.00956
49. Tang J, Lu L, Liu Y, et al. Quercetin improve ischemia/reperfusion-induced cardiomyocyte apoptosis in vitro and in vivo study via SIRT1/PGC-1α signaling. *J Cell Biochem*. 2019;120(6):9747–9757. doi:10.1002/jcb.28255
50. Suchal K, Malik S, Gamad N, et al. Kaempferol attenuates myocardial ischemic injury via inhibition of MAPK signaling pathway in experimental model of myocardial ischemia-reperfusion injury. *Oxid Med Cell Longev*. 2016;2016:7580731. doi:10.1155/2016/7580731
51. Wang D, Zhang X, Li D, et al. Kaempferide protects against myocardial ischemia/reperfusion injury through activation of the PI3K/Akt/GSK-3β pathway. *Mediators Inflamm*. 2017;2017:5278218. doi:10.1155/2017/5278218

52. Zhou M, Ren H, Han J, Wang W, Zheng Q, Wang D. Protective effects of kaempferol against myocardial ischemia/reperfusion injury in isolated rat heart via antioxidant activity and inhibition of glycogen synthase kinase-3β. *Oxid Med Cell Longev*. 2015;2015:481405. doi:10.1155/2015/481405
53. Liang W, Huang X, Chen W. The effects of baicalin and baicalein on cerebral ischemia: a review. *Aging Dis*. 2017;8(6):850–867. doi:10.14336/ad.2017.0829
54. Yang S, Wang H, Yang Y, et al. Baicalein administered in the subacute phase ameliorates ischemia-reperfusion-induced brain injury by reducing neuroinflammation and neuronal damage. *Biomed Pharmacother*. 2019;117:109102. doi:10.1016/j.biopha.2019.109102
55. Song L, Yang H, Wang HX, et al. Inhibition of 12/15 lipoxygenase by baicalein reduces myocardial ischemia/reperfusion injury via modulation of multiple signaling pathways. *Apoptosis*. 2014;19(4):567–580. doi:10.1007/s10495-013-0946-z
56. Luan Y, Sun C, Wang J, et al. Baicalin attenuates myocardial ischemia-reperfusion injury through Akt/NF-κB pathway. *J Cell Biochem*. 2019;120(3):3212–3219. doi:10.1002/jcb.27587
57. Zhao L, Zhou Z, Zhu C, Fu Z, Yu D. Luteolin alleviates myocardial ischemia reperfusion injury in rats via Siti1/NLRP3/NF-κB pathway. *Int Immunopharmacol*. 2020;85:106680. doi:10.1016/j.intimp.2020.106680
58. Hu Y, Zhang C, Zhu H, et al. Luteolin modulates SERCA2a via Sp1 upregulation to attenuate myocardial ischemia/reperfusion injury in mice. *Sci Rep*. 2020;10(1):15407. doi:10.1038/s41598-020-72325-8
59. Lin F, Xu L, Huang M, et al. β-Sitosterol protects against myocardial ischemia/reperfusion injury via targeting PPARγ/NF-κB signalling. *Evid Based Complement Alternat Med*. 2020;2020:2679409. doi:10.1155/2020/2679409
60. Halladin NL. Oxidative and inflammatory biomarkers of ischemia and reperfusion injuries. *Dan Med J*. 2015;62(4):B5054.
61. Liu A, Wan A, Feng A, Rui R, Zhou B. ICAM-1 gene rs5498 polymorphism decreases the risk of coronary artery disease. *Medicine*. 2018;97(40):e12523. doi:10.1097/md.0000000000012523
62. Hausenloy DJ, Yellon DM. Myocardial ischemia-reperfusion injury: a neglected therapeutic target. *J Clin Invest*. 2013;123(1):92–100. doi:10.1172/jci62874
63. Hassanzadeh-Makoui R, Razi B, Aslani S, Imani D, Tabaee SS. The association between Matrix Metallo-proteinases-9 (MMP-9) gene family polymorphisms and risk of Coronary Artery Disease (CAD): a systematic review and meta-analysis. *BMC Cardiovasc Disord*. 2020;20(1):232. doi:10.1186/s12872-020-01510-4
64. Nitulescu GM, Van De Venter M, Nitulescu G, et al. The Akt pathway in oncology therapy and beyond (Review). *Int J Oncol*. 2018;53(6):2319–2331. doi:10.3892/ijo.2018.4597
65. Sussman MA, Völkers M, Fischer K, et al. Myocardial AKT: the omnipresent nexus. *Physiol Rev*. 2011;91(3):1023–1070. doi:10.1152/physrev.00024.2010